

Accepted Manuscript

Synthesis of novel 7-azaindole derivatives containing pyridin-3-ylmethyl dithiocarbamate moiety as potent PKM2 activators and PKM2 nucleus translocation inhibitors

Bin Liu, Xia Yuan, Bo Xu, Han Zhang, Ridong Li, Xin Wang, Zemei Ge, Runtao Li



PII: S0223-5234(19)30214-4

DOI: <https://doi.org/10.1016/j.ejmech.2019.03.003>

Reference: EJMECH 11173

To appear in: *European Journal of Medicinal Chemistry*

Received Date: 28 December 2018

Revised Date: 19 February 2019

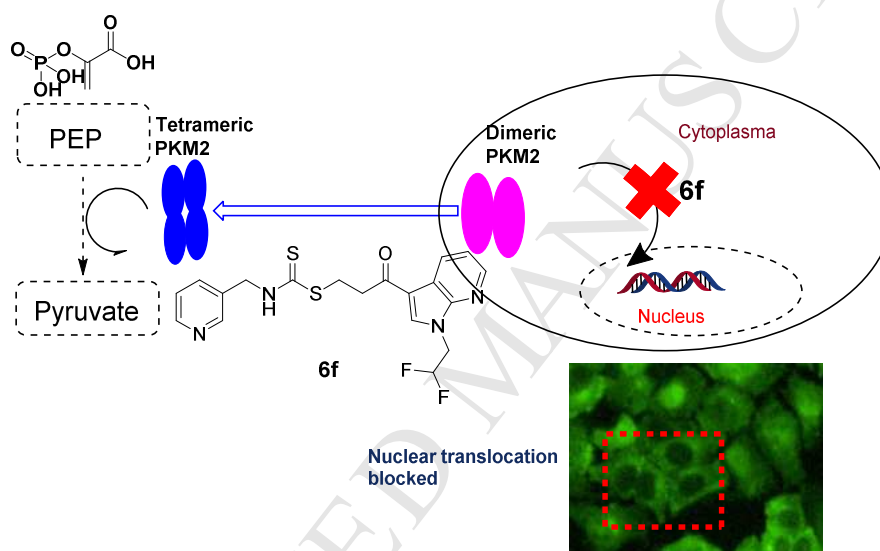
Accepted Date: 1 March 2019

Please cite this article as: B. Liu, X. Yuan, B. Xu, H. Zhang, R. Li, X. Wang, Z. Ge, R. Li, Synthesis of novel 7-azaindole derivatives containing pyridin-3-ylmethyl dithiocarbamate moiety as potent PKM2 activators and PKM2 nucleus translocation inhibitors, *European Journal of Medicinal Chemistry* (2019), doi: <https://doi.org/10.1016/j.ejmech.2019.03.003>.

This is a PDF file of an unedited manuscript that has been accepted for publication. As a service to our customers we are providing this early version of the manuscript. The manuscript will undergo copyediting, typesetting, and review of the resulting proof before it is published in its final form. Please note that during the production process errors may be discovered which could affect the content, and all legal disclaimers that apply to the journal pertain.

Synthesis of novel 7-azaindole derivatives containing pyridin-3-ylmethyl dithiocarbamate moieties as potent PKM2 activators and PKM2 nucleus translocation inhibitors

Graphical abstract



Synthesis of novel 7-azaindole derivatives containing pyridin-3-ylmethyl dithiocarbamate moiety as potent PKM2 activators and PKM2 nucleus translocation inhibitors

Bin Liu^{†,a}, Xia Yuan^{†,a}, Bo Xu^a, Han Zhang^a, Ridong Li^{a,b}, Xin Wang^a, Zemei Ge^{a,*},
Runtao Li^{a,*}

^a State Key Laboratory of Natural and Biomimetic Drugs, School of Pharmaceutical Sciences, Peking University, Beijing 100191, China.

^b Institute of Systems Biomedicine, School of Basic Medical Sciences, Peking University, Beijing 100191, China.

[†] These authors contributed equally.

* Corresponding authors; email: zmge@bjmu.edu.cn; lirt@bjmu.edu.cn.

Abstract

Multiple lines of evidence have indicated that pyruvate kinase M2 (PKM2) is upregulated in most cancer cells and it is increasingly recognized as a potential therapeutic target in oncology. In a continuation of our discovery of lead compound **5** and SAR study, the 7-azaindole moiety in compound **5** was systematically optimized. The results showed that compound **6f**, which has a difluoroethyl substitution on the 7-azaindole ring, exhibited high PKM2 activation potency and anti-proliferation activities on A375 cell lines. In a xenograft mouse model, oral administration of compound **6f** led to significant tumor regression without obvious toxicity. Further mechanistic studies revealed that **6f** could influence the translocation of PKM2 into nucleus, as well as induction of apoptosis and autophagy of A375 cells. More importantly, compound **6f** significantly inhibited migration of A375 cells in a concentration-dependent manner. Collectively, **6f** may serve as a lead compound in the development of potent PKM2 activators for cancer therapy.

Keywords: PKM2; Structure-Activity Relationships; Nuclear Translocation; Apoptosis; Autophagy

1. Introduction

Cancer is currently the leading cause of death globally [1-3]. Over the past decades, cancer therapeutic drugs via various anti-cancer mechanisms are approved [4-6]. Recently, targeting cancer metabolism has become a valid strategy in the development of new tumor treatments [7-9]. In 2017, FDA approved Enasidenib (AG-221), an inhibitor of mutant isocitrate dehydrogenase 2 (IDH2) protein, for the treatment of relapsed or refractory acute myeloid leukemia [10].

In addition to IDH, the pyruvate kinase M2 (PKM2) has also emerged as a critical regulator in cancer cell metabolism. In the 1920s, Otto Warburg found that most cancer cells produce energy by a high rate of glycolysis followed by lactic acid fermentation in the cytoplasm, despite the availability of oxygen, known as Warburg Effect [11]. Pyruvate kinase (PK) regulates the final rate-limiting step of glycolysis and converts phosphoenolpyruvate (PEP) to pyruvate while phosphorylating ADP to ATP. Although, there are four isoforms of PK in mammalian cells [12-13], named PKL, PKR, PKM1 and PKM2, only PKM2 is necessary for cancer metabolism and tumor growth [14-19]. This finding is further supported by the research that when PKM2 was replaced with PKM1, the constitutively active PKM1 delayed xenograft tumor growth [20]. Moreover, PKM1 as a fully active tetramer acts only to maximize the efficiency of glycolysis. Unlike PKM1, PKM2 acts as a key regulator in maintaining the balance between the energy needs (tetramer) and building block needs for increasing biomass (dimer) [21-23]. It has been demonstrated that restoring the activity of PKM2 (dimer) to PKM1-like levels (tetramer) may cause cancer cells to revert to a metabolic state like that of normal cells [24]. Therefore, fixation of PKM2 in its active tetrameric form by activators may have the therapeutic potential for the treatment of cancer.

Up till now, several PKM2 activators have been reported [25-37]. In 2010, two PKM2 activators *N,N'*-diarylsulfonamide (**1**) [27] and thieno[3,2-*b*]pyrrole[3,2-*d*]-pyridazinone (**2**) [29] were first reported (**Fig. 1**). Structural studies revealed that these two activators bind PKM2 at the subunit interaction interface, which is different

from that of the endogenous activator fructose-1,6-bisphosphate (FBP) [26]. In addition, another interesting scaffold quinoline sulfonamide **3**, which adopted a unique and different binding mode from compound **1** or **2**, was also discovered by Dang's group [31]. In spite of these discoveries, none of these compounds had an inhibitory effect on tumor cell proliferation, unless the tumor cell assay was performed under hypoxic condition [26, 30] or in models where non-essential amino acids such as serine were stripped [21, 31]. More recently, while our paper was in preparation, Chen and co-workers reported a natural product micheliolide **4** (MCL) which could irreversibly activate PKM2 and suppress the growth of leukemia cells through reducing its nuclear translocation [38]. Our groups recently have also reported a novel 7-azaindole derivative containing pyridin-3-ylmethyl dithiocarbamate moiety **5** as a potent PKM2 activator, which was obtained by screening our in-house compound library [39]. Interestingly, this series of activators could strongly inhibit cellular growth in tumor cell lines, while maintaining low toxicities towards non-cancer cell lines. Moreover, compound **5** has high selectivity towards PKM2 versus other PK isoforms, such as PKM1 and PKR. In this work, we report the optimization of compound **5** and investigation of its unique mechanism in regulating PKM2 nuclear translocation. Our efforts led to the discovery of compound **6f** as a promising PKM2 activator with both *in vitro* and *in vivo* antitumor activity.

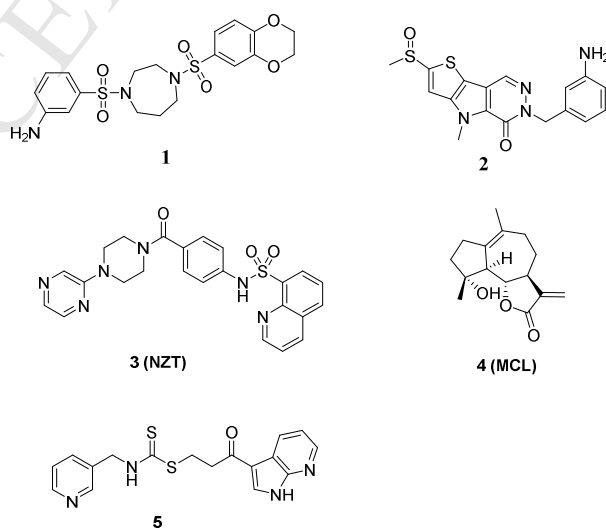


Fig. 1. Structures of representative PKM2 activators

2. Results and Discussion

2.1. Optimization strategy

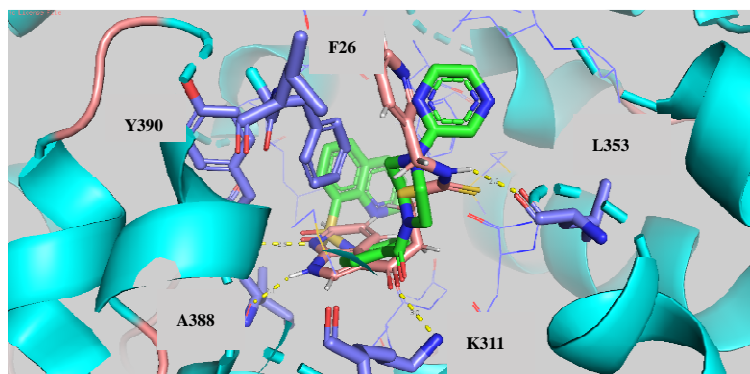
In order to understand the binding mechanism for guidance of optimization, the molecular docking of compound **5** with PKM2 was performed using the co-crystal structure of **3** (also called **NZT**, PDB:4G1N), as we anticipate these two molecules may share a similar binding mode [31, 39]. As shown in **Fig. 2**, compound **5** could align well with **NZT**, and the azaindole moiety is caged among residues Phe26, Leu27, Met30 and Tyr390 from chain A. The pyridinyl group is packed between residues Phe26 and Leu 394 in chain B. Moreover, the 7-nitrogen in the azaindole ring forms a hydrogen bond with Tyr390A. The carbonyl group in the compound is found to interact with the side chain of Lys311B through hydrogen bonding, which highly simulates the function of the same group of **NZT**. Furthermore, there is a π - π staking interaction between the 7-azaindole ring and Phe26A.

We had previously demonstrated that the pyridin-3-ylmethanamine moiety provides several advantages such as improved PKM2 potency (**Fig. 2A**) and selectivity [32, 39]. Therefore, we elected to keep this core structure intact. In addition, the docked model showed that there seems little space for the modification on the pyridin-3-ylmethanamine ring (**Fig. 2B**). Based on the docking results and the preliminary SAR from HTS, the optimization for lead compound **5** was focused on the azaindole ring of the molecule and was divided into three parts.

Substitution of 1-nitrogen of 7-azaindole ring

Although, 1-nitrogen of 7-azaindole ring forms a hydrogen bond with Ala388 (**Fig. 2A**), we believe that this hydrogen bond interaction is dispensable, and there are some room here for substituent groups. The modified compounds may be still active when the interaction is blocked by the appropriate groups.

A



B

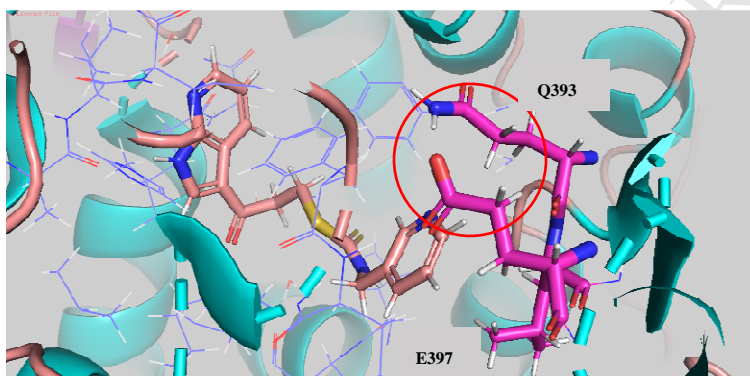


Fig. 2. A. Predicted binding mode of compound **5** with PKM2 (cartoon). NZT is shown in green sticks and compound **5** is shown in pink sticks. Key residues are shown in purple sticks. Yellow dotted lines are hydrogen bond interactions; **B.** Possible clash residues in red circle.

Introduction of substitutions on 7-azaindole ring

The docking results revealed that there are some spaces inside the pocket formed between PKM2 and the 7-azaindole scaffold, and the inner pocket might fit a bulkier group for enhanced hydrophobic interactions. We therefore planned to introduce substitutions, especially hydrophobic groups, to the 4th-6th position of 7-azaindole ring for increased binding affinity.

Replacing 7-azaindole ring with 7-azaindole-like heterocyclic rings

We explored some 7-azaindole-like heterocyclic rings that may show higher binding potency to PKM2 than 7-azaindole.

2.2. SAR investigation and anti-proliferation activities

All the synthesized compounds were firstly evaluated for the cell-free PKM2

activation activity *via* a previously reported assay [39]. These compounds with higher PKM2 activation activity were further examined for their anticancer activities.

Various substitutions were introduced onto the 1-nitrogen of 7-azaindole ring to form the corresponding compounds **6a-6f**. As shown in Table 1, all the target compounds exhibited moderate to excellent PKM2 activation activity (2.50 - 4.56 μM) except compound **6e**. This result shows that our initial prediction is reasonable, though the PKM2 activation potency is slightly decreased comparing with the lead **5** ($\text{AC}_{50} = 1.0 \mu\text{M}$). 1-Phenyl substituted compound (**6d**, $\text{AC}_{50} = 2.50 \mu\text{M}$) exhibited higher activity than 1-thiophene substituted compound (**6e**, $\text{AC}_{50} > 20 \mu\text{M}$), which demonstrated that different substituents on the 1st position had different effects on the activity. Notably, when the 1-methyl group of **6a** was replaced by 1,1-difluoroethyl, the corresponding compound **6f** ($\text{R}^1 = -\text{CH}_2\text{CF}_2\text{H}$) not only exhibited better activity ($\text{AC}_{50} = 2.67 \mu\text{M}$), but also showed the highest activation (149%). Therefore, compound **6f** was also docked into the above model (**Fig. 3**), as can be seen, 1,1-difluoroethyl group could be well adapted in the binding pocket without large steric clashes. This preliminary exploration resulted in some satisfying outcome and verified that the hydrogen bond interaction with A388 is not absolutely required.

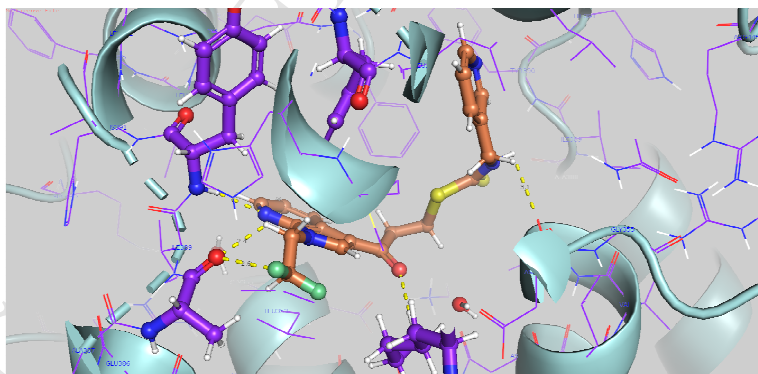
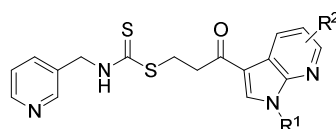


Fig. 3. Predicted binding mode of compound **6f** (orange sticks) with PKM2 (cartoon). Key residues are shown in purple sticks. Yellow dotted lines are hydrogen bond interactions;

For the substitution modification on 7-azaindole ring, the 4 or 5-halogen substituted analogues (**6h**, $\text{AC}_{50} = 0.61 \mu\text{M}$; **6l**, $\text{AC}_{50} = 0.18 \mu\text{M}$) greatly enhanced the activity of PKM2. The possible reason may be the increased hydrophobic interactions based on the docking results. Moreover, the electron-withdrawing effect of the halogen may also contribute to the stronger hydrogen bond interaction between 7-nitrogen and

Y390. Unfortunately, when 7-azaindole was substituted with other hydrophobic groups at the 4th or 5th position (**6i-6k**, **6m**), the activity was significantly decreased, suggesting that large groups on these positions had detrimental effect. 6-Substituted 7-azaindole derivatives with halogen or methyl (**6n**, **6o**) led to complete loss of binding affinity with PKM2 ($AC_{50} > 20 \mu M$) in comparison with the unsubstituted derivative **5**.

Table 1. *In vitro* PKM2 activation activity of 7-azaindole derivatives

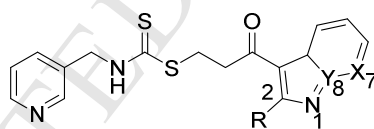


Compd.	R ¹	R ²	AC ₅₀ ^a / μM ^b	Max (%)
5	H	H	1.00	113
6a	Me	H	4.35	114
6b	<i>cyclo</i> -Bu	H	3.93	93
6c	<i>cyclo</i> -Pr	H	4.56	42
6d	1-Ph	H	2.50	77
6e	2-Thiophenyl	H	NA ^c	NA
6f	-CH ₂ CF ₂ H	H	2.67	149
6g	H	4-Cl	1.14	122
6h	H	4-Br	0.61	83
6i	H	4- <i>cyclo</i> -Pr	NA	NA
6j	H	4-Ethyne	>20	24
6k	H	4-Ph	2.17	28
6l	H	5-Cl	0.18	71
6m	H	5-Cl-Ph	> 20	NA
6n	H	6-Cl	NA	NA
6o	H	6-Me	NA	NA

^a AC₅₀ = half maximal active concentration; ^b Data are expressed as the mean of at least two determinations; ^c NA = Not active on PKM2;

In order to further explore the structure-activity relationships, we moved 7-nitrogen from compound **5** to 8-nitrogen to afford compound **15a** and replaced 8-carbon in compound **5** with nitrogen atom to obtain compound **15b**. Comparing with compound **5** (Table 2), the PKM2 activation potency of **15a** was completely abolished ($AC_{50} > 20 \mu\text{M}$). However, the PKM2 activation potency of **15b** was greatly improved by about 4 to 5 times ($AC_{50} = 0.22 \mu\text{M}$), though the maximum response was moderate (Max = 44%). Encouraged by the excellent PKM2 activation activity of **15b**, we then synthesized compound **15c** by introducing phenyl onto 2nd-position of **15b**. We found that **15c** ($AC_{50} = 0.45 \mu\text{M}$, Max = 148%) did not only maintain the activation potency, but also significantly increase the maximal activity. The docking results showed that 2-phenyl could make additional π - π staking interactions with Phe26B (**Figure S1**). These results suggested that the nitrogen at 7-position is very important for activity and the introduction of substitute at 2-position may improve the maximal response activity.

Table 2. *In vitro* PKM2 activation activity of heterocycle derivatives



Compd.	X	Y	R	$AC_{50}/\mu\text{M}^a$	Max (%)
5	N	C	H	1.00	113
15a	C	N	H	>20	23
15b	N	N	H	0.22	44
15c	N	N	Ph	0.45	148

^aData are expressed as the mean of at least two determinations;

Compounds with higher PKM2 activation activity were subsequently evaluated for their inhibitory activities against PKM2 high expression cell lines, H1299 (human lung cancer), HCT116 (human colon cancer) and A375 (human melanoma cancer). As illustrated in Table 3, all of them showed robust tumor inhibition, especially on A375

cell line, and their IC₅₀ values ranged from 3.86 to 0.21 μM. Several 7-azaindole analogues (**6a**, **6c**, **6f** and **6g**) were more potent than the lead compound **5**. Among them, **6f** was the best one with IC₅₀ values of 2.29, 0.71, and 0.28 μM against H1299, HCT116 and A375 cell lines, respectively. Comparing the anti-proliferation activities of compounds **5** with **15b**, it is clear that the pyrazolopyridazine scaffold was also a good starting point for further optimization.

Table 3. Inhibition of cell growth of H1299, HCT116 and A375 cell lines

Compd.	Antiproliferation / IC ₅₀ (μM) ^a		
	H1299	HCT116	A375
5	3.68 ± 0.40	3.09 ± 0.97	1.03 ± 0.07
6a	2.09 ± 0.07	0.94 ± 0.11	0.29 ± 0.10
6b	4.20 ± 1.68	3.52 ± 0.25	1.34 ± 0.01
6c	9.51 ± 0.41	0.84 ± 0.10	0.21 ± 0.01
6d	10.03 ± 1.53	5.36 ± 0.47	3.86 ± 1.58
6f	2.28 ± 0.08	0.71 ± 0.01	0.28 ± 0.09
6g	2.50 ± 0.35	2.06 ± 0.45	0.41 ± 0.08
6h	>10	4.90 ± 1.13	1.99 ± 0.40
6l	8.87 ± 0.52	6.16 ± 0.51	3.38 ± 0.24
15b	1.76 ± 0.91	1.52 ± 0.18	0.33 ± 0.08
15c	>10	9.08 ± 0.69	2.77 ± 0.36

^aData are average of three independent experimental measurements and expressed as Mean ±SD

Finally, we selected **6f** for further investigation owing to its high PKM2 activation potency (highest activation) and excellent anti-proliferation activity. First, the toxicities of **6f** on non-cancer cells were tested. As shown in Table 4, it showed low toxicities on Helf (human embryonic lung fibroblast) and C2C12 (mouse myoblast) cell lines. Second, due to the many structural similarities between compound **6f** and B-raf kinase inhibitor vemurafenib, **6f** was also tested on the effect against serine-threonine kinase B-raf in a single-point binding at 10 μM (Table 4). It displayed low inhibition (41%) compared with vemurafenib, confirming that

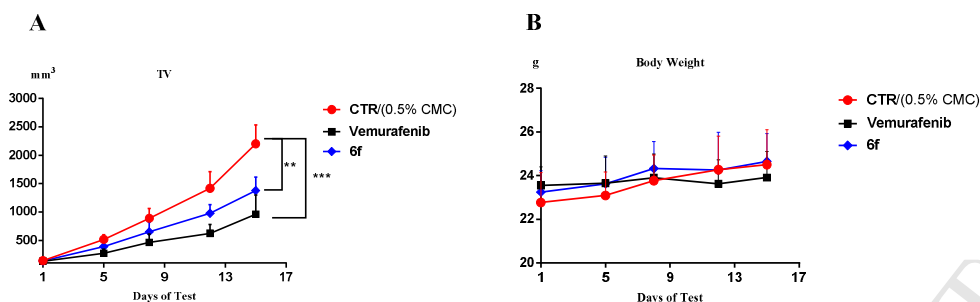
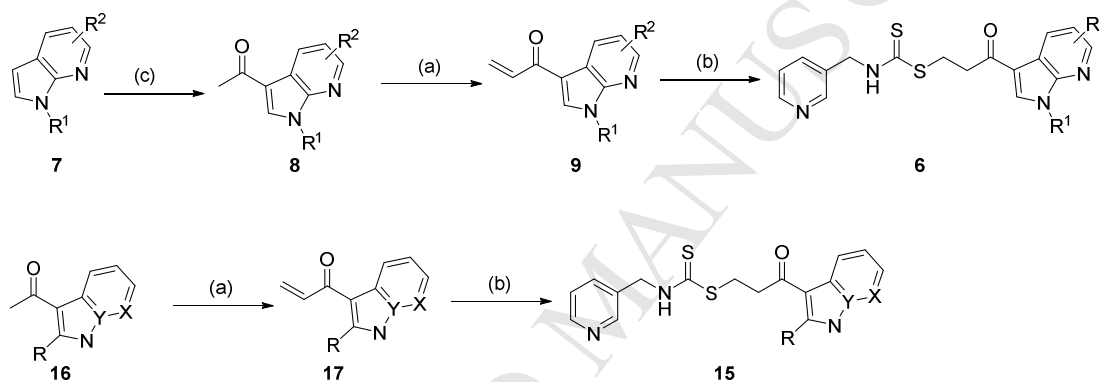


Fig. 4. **6f** inhibits tumor growth *in vivo*. (A) Tumor growth curves in mice receiving the respective treatments by tumor volume. (B) Average body weight of mice. **, $P < 0.01$; ***, $P < 0.001$.

2.4. Synthetic Chemistry



Scheme 1. General synthetic routes for compounds **6** and **15**. Reagents and conditions: (a) $(\text{HCHO})_n$, CF_3COOH , $(i\text{Pr})_2\text{NH}$, DMF, 90°C , 24 h; (b) 3-(aminomethyl)pyridine, CS_2 , TEA, DMF, rt, 6 h; (c) AlCl_3 , DCM, then $\text{NaOH}(1\text{N})$.

All the new derivatives were synthesized following the general synthetic routes shown in Scheme 1. Acetylation of substituted 7-azaindole derivatives (**7**) gave the 3-acetyl-7-azaindole derivatives (**8**). Treatment of acetoxyated heterocycles (**8** and **16**) with paraformaldehyde catalyzed by diisopropylammonium trifluoroacetate afforded the intermediates acryloyl heterocycles (**9** and **17**), which were further treated with dithiocarbamates generated from CS_2 and 3-(aminomethyl)pyridine to yield the corresponding target compounds (**6** and **15**), respectively. Therefore, the key steps were the preparations of starting materials of substituted 7-azaindole analogues (**7a-7o**) and acetoxyated heterocycles (**16a-16c**).

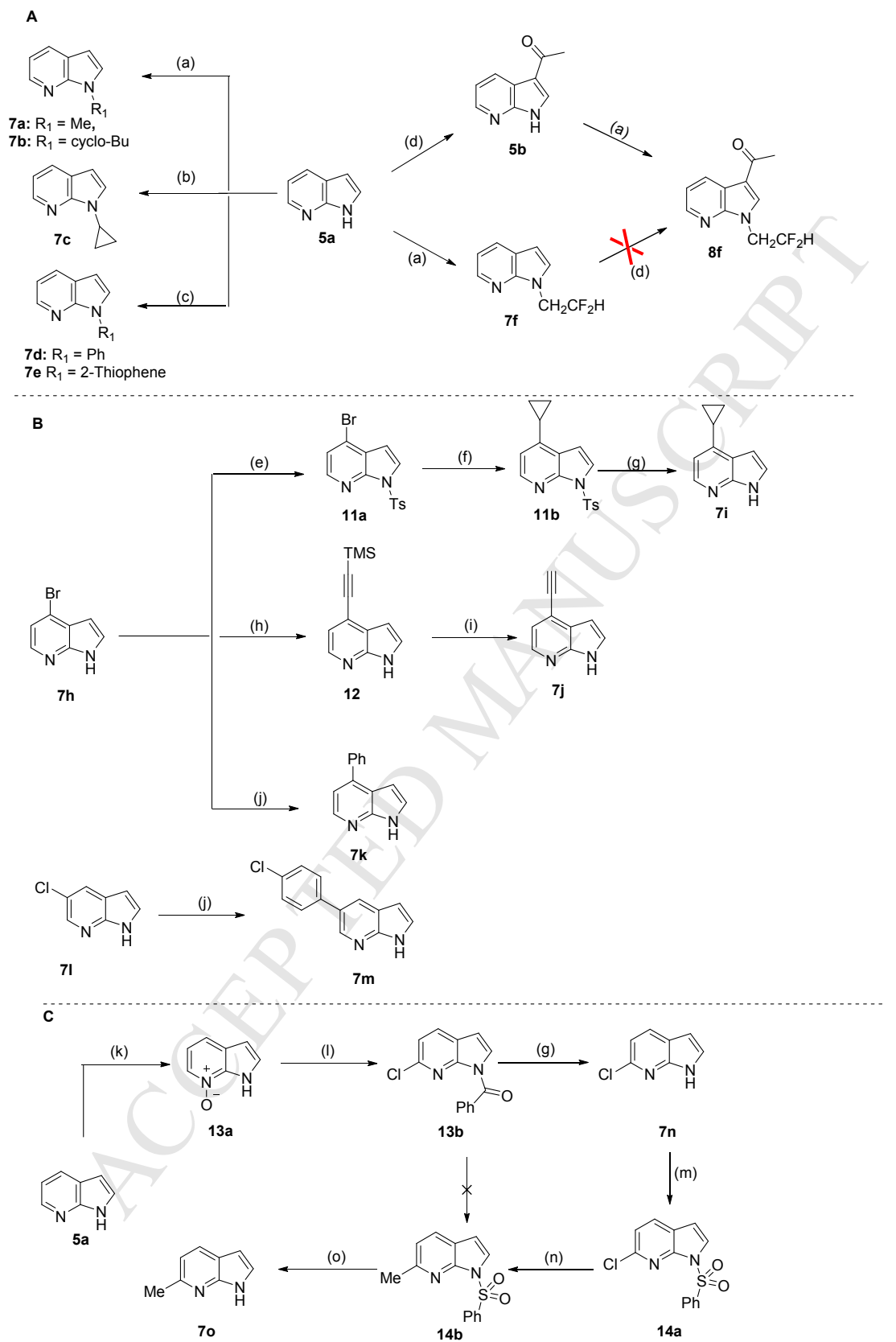
Preparation of **7a-7o**

1-Substituted 7-azaindole **7a-7f** could be achieved *via* a $\text{S}_{\text{N}}2$ or Ullman C-N

coupling reactions (Scheme 2A). The formation of **7f** could not occur via the Friedel-Crafts reaction due to the influence of 1,1-difluoroethyl at 1-N position. Therefore, **8f** was prepared from the N-alkylation of acetylated 7-azaindole **5b** (Scheme 2A). Alternatively, 4- or 5- substituted derivatives (**7i-7k**) were prepared through Suzuki or Sonogashira reactions of commercially available 4-Br-7-azaindole **7h** (or 5-Cl-7-azaindole, **7l**) with corresponding boronic acid or TMS protected acetylene (Scheme 2B). For the synthesis of 7-azaindole scaffold **7n** and **7o**, 7-azaindole **5a** was oxidized by *m*-CPBA to give 7-azaindole N-oxide **13a**, which was treated with acid halides to give the intermediate **13b**. Acyl groups are readily removed under basic conditions to get **7n** [40]. Protection of indole NH as sulfonamide (**7n** to **14a**), followed by palladium catalyzed Negishi cross-coupling with MeZnCl was carried out to introduce the 6-methyl group in 7-azaindole (**14b**) [41]. After the protecting group was removed, intermediate **7o** was obtained smoothly (Scheme 2C). Other substituted 7-azaindoles were commercially available.

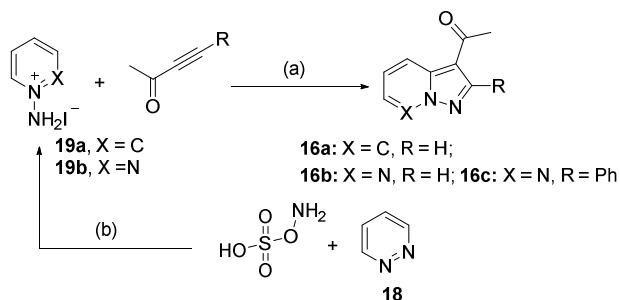
Preparation of 16a-16c

The synthetic routes for the acetylated heterocycles **16a-16c** are depicted in Scheme 3 according to the published papers [42-43]. For the construction of pyrazolo[1,5-a]pyridinyl **16a**, 1-aminopyridinium iodide (**19a**) was reacted with 3-butyne-2-one through 1,3-dipolar cycloaddition under basic conditions to give the target molecule. Alternatively, pyridazine (**18**) was treated with hydroxylamine O-sulfonic acid to afford the intermediate **19b**, which was further converted into **16b-16c** by the same routes.



Scheme 2. Synthesis of key intermediates **7a-7o** and **8f**. Reagents and conditions: (a) NaH, THF, 0°C or Cs₂CO₃, DMF, 70 °C; (b) *cyclo*-PrB(OH)₂, Cu(OAc)₂, Bipy, Na₂CO₃, DCE; (c) PhI or 2-I-thiophene, CuI, K₃PO₄, Ethane-1,2-diamine, 1,4-dioxane, reflux; (d) AlCl₃, DCM, then NaOH(1N); (e) TosCl, TBHS, NaOH(aq), DCM; (f)

cyclo-PrB(OH)₂, Pd(OAc)₂, X-Phos, Cs₂CO₃, toluene/H₂O; (g) 4N NaOH, MeOH; (h) TMS–ethyne, CuI, Pd(PPh₃)Cl₂, TEA; (i) 1N NaOH, MeOH; (j) Pd(PPh₃)₄, Cs₂CO₃, dppf, 1,4-dioxane/H₂O, ArB(OH)₂; (k) *m*-CPBA, EtOAc; (l) PhCOCl, HMDS, toluene; (m) PhSO₂Cl, NaOH(aq), TBHS, DCM; (n) Pd(PPh₃)₄, MeZnCl, THF, 80 °C; (o) 2N NaOH(aq), EtOH, reflux.



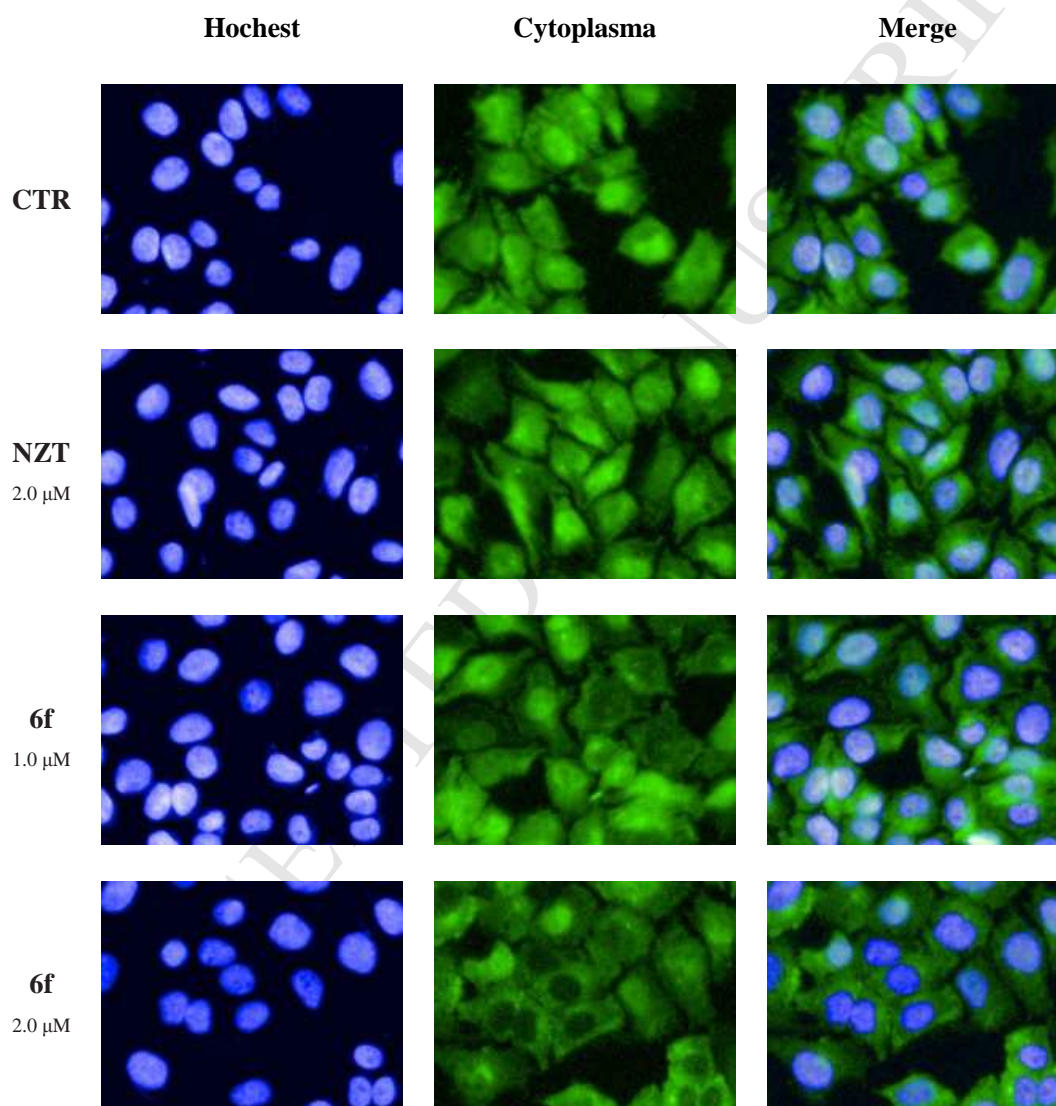
Scheme 3. Synthesis of key intermediates **16a-16c**. Reagents and conditions: (a) KOH, K₂CO₃, DMSO; (b) KHCO₃, KOH, H₂O.

2.5. Compound **6f** reduces the nuclear translocation of PKM2

Recently, Yang *et al.* has demonstrated that the nuclear function of PKM2 contributes to cell proliferation *via* EGFR activation pathway [44-46]. Furthermore, when PKM2 fails to translocate to the nucleus, EGF-promoted Warburg effect could be impaired, suggesting that the antitumor activity of some PKM2 activators may also arise from inhibition of PKM2's nuclear function [47-48]. Sizemore *et al.* also found that PKM2 could regulate homologous recombination mediated DNA double-strand break repair through its nuclear accumulation [49]. More recently, Li's group found that compound **5** (**MCL**) could activate PKM2, inhibit the acetylation of lysine433, and finally influence the translocation of PKM2 into nucleus [38]. To demonstrate whether compound **6f** could inhibit the translocation of PKM2, an immunofluorescence assay was performed with compound **NZT** as the control. **Fig. 5A** revealed that only **6f** treatment for 24 h resulted in retardation of the nuclear accumulation of PKM2 in A375 cells in a concentration-dependent manner. The percentage of immunofluorescence intensity (cytoplasm) in **6f** 2.0 μM group was significantly lower than that in CTR group (**Fig. 5B**, $p < 0.05$). Because most cells died after treatment with 4.0 μM **6f** for 24 h, a 12 h immunofluorescence assay was performed. As shown in **Figure S2**, an obvious reduction of the nuclear translocation of PKM2 was also observed after treatment with **6f**. All of these results demonstrated

that **6f** could effectively reduce PKM2 nuclear translocation, and further suppress tumorigenesis. Inhibition of PKM2 nuclear translocation may be one of the key reasons why **6f** not only exhibited high PKM2 activity, but also showed robust anti-proliferation effect on tumor cells both *in vitro* and *in vivo* (Other unknown activities of **6f** may also be contributing to the effects on tumor growth.).

A



B

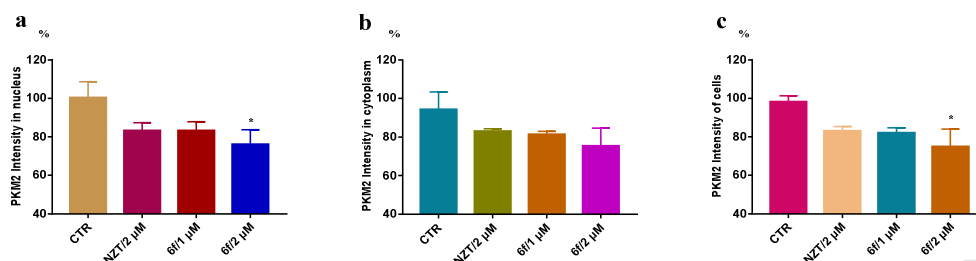


Fig. 5. **6f** inhibits PKM2 translocation into the nucleus. (A) High content screening immunofluorescence microscopy was performed to analyze localization of PKM2 in A375 cells after treatment with **NZT** or **6f** for 24 h; PKM2 was labeled with antibody, DNA was visualized with Hoechst (blue) (B) Average immunofluorescence intensity; a) Intensity in nucleus; b) Intensity in cytoplasm; c) Intensity of cells. *, $P < 0.05$.

2.6. Compound **6f** could induce cellular apoptosis and autophagy

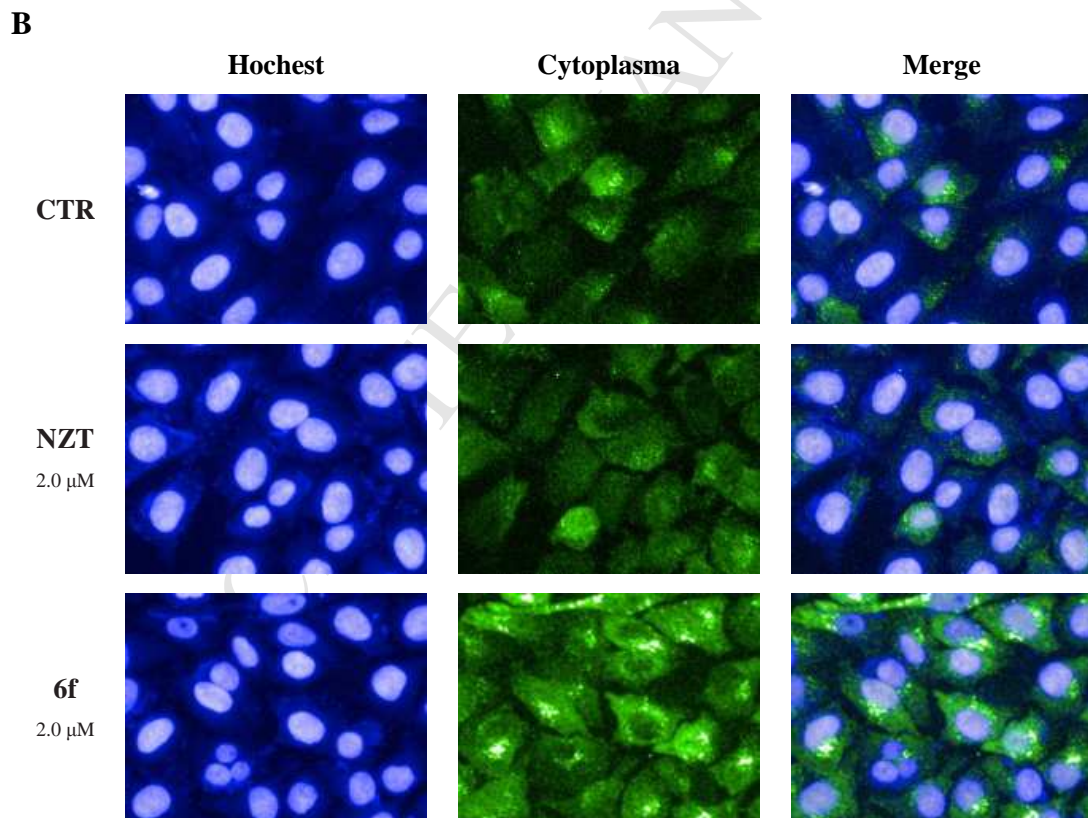
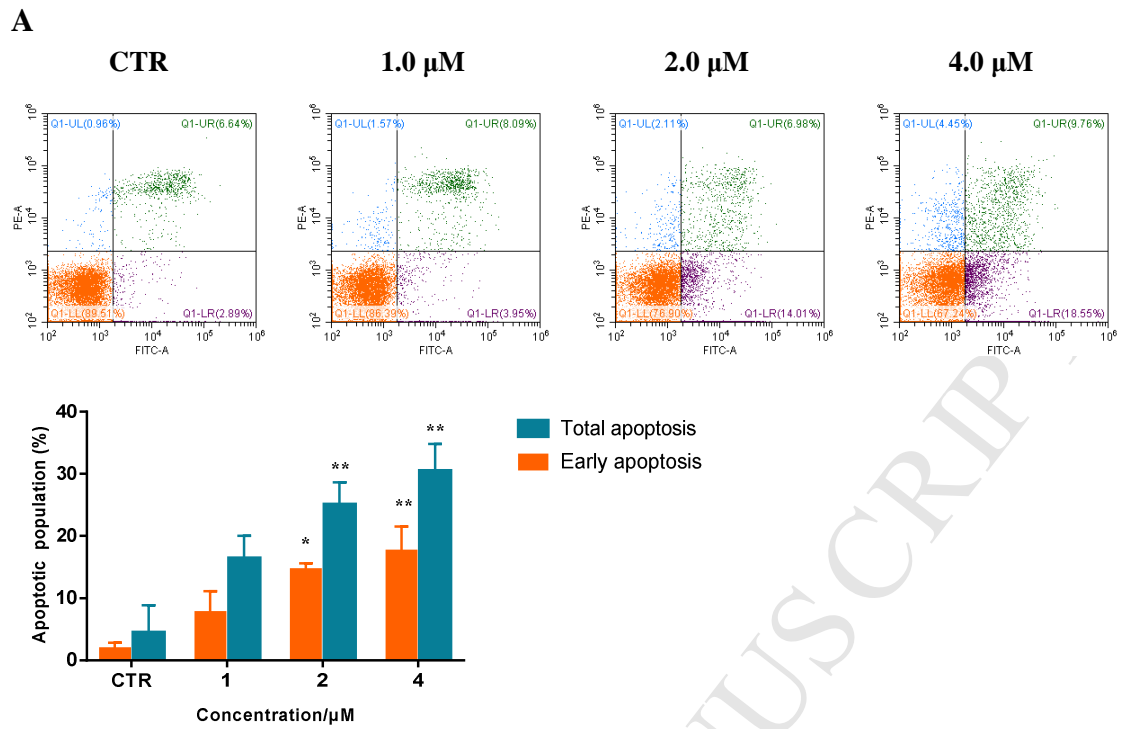
Since PKM2 regulates the apoptotic activity and inhibits autophagy [50-52], which contribute to the development of malignant cancer, compound **6f** might induce cellular apoptosis and promote autophagy. The annexin-V/PI double staining assay was applied to determine the number and stage of apoptotic A375 cells after treated with **6f** using flow cytometry. As shown in **Fig. 6A**, treatment of A375 cells with compound **6f** for 24 h led to a concentration-dependent apoptosis, and the percentages of apoptotic cells were 12.0%, 21.0% and 28.3%, respectively. Specially, when treated with **6f** at 2.0 and 4.0 μM , the numbers of apoptotic cells were remarkably higher than that of the control group ($P < 0.05$). Since the transition of LC3-I to LC3-II is an imperative step in autophagy and the number of LC3B puncta represents the number of autophagosomes, we utilized immunofluorescence staining (high content screening) to analyze whether autophagy was involved in the process of cell death induced by **6f** (**Fig. 6B**). Treatment of A375 cells with **6f** resulted in substantial increase in LC3B fluorescence intensities compared to DMSO control (**Fig. 6C**), consistent with other related indicators, such as LC3B spot area. Thus, it demonstrated that **6f** could also promote cellular autophagy in a concentration-dependent manner.

2.7. Effects of compound **6f** on tumor cell migration

Recent studies have shown that PKM2 is associated with the migration and evasion of cancer cells [52]. The effects of compound **6f** on tumor cell migration were assessed using living cell high content screening workstations. As displayed in **Fig. 7A** and **7B**, after treatment with compound **6f** for 24 h, both the migration speed and accumulated distance of A375 cells were significantly inhibited in a concentration-dependent manner. These results demonstrated that **6f** could efficiently exhibit antimetastatic potential against cancer cells. Meanwhile, the proliferation rate of A375 cells could also be determined, which is in accordance with the previously determined IC_{50} (**Fig. 7C**).

3. Conclusion

A series of derivatives of **5** were designed and synthesized to optimize the 7-azaindole moiety. Several compounds were found to show potent PKM2 activation activity and high inhibitory activity on tumor cell lines. A representative compound **6f** was selected for further study. Compound **6f** exhibited high proliferation inhibitory activity *in vitro*, and significant anticancer activity *in vivo*. The preliminary mechanism studies showed that **6f** effectively inhibited the translocation of PKM2 into the nucleus, which may be one of the key mechanisms for its role in inhibiting proliferation. The results also showed that compound **6f** could induce cellular apoptosis, promote autophagy, and strongly inhibit the migration of A375 cells in a concentration-dependent manner. The pharmacokinetics and safety studies of **6f** are currently underway.



C

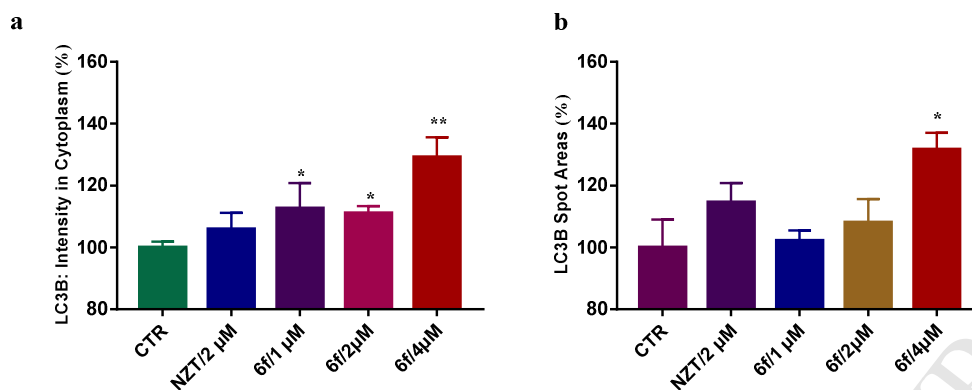


Fig. 6. (A) **6f** induced apoptosis in A375 cells. A375 cells were harvested after treatment with various concentrations of **6f** or DMSO for 24 h; (B) Immunofluorescence staining of A375 cells showing the appearance of autophagosomes. Immunofluorescence staining of A375 cells treated with DMSO or **6f** for 24 h, LC3B was labeled with antibody (green), and DNA was visualized with Hoechst (blue); (C) Average immunofluorescence intensity or areas; a) LC3B intensity in cytoplasm; b) LC3B spot areas; *, $P < 0.05$; **, $P < 0.01$.

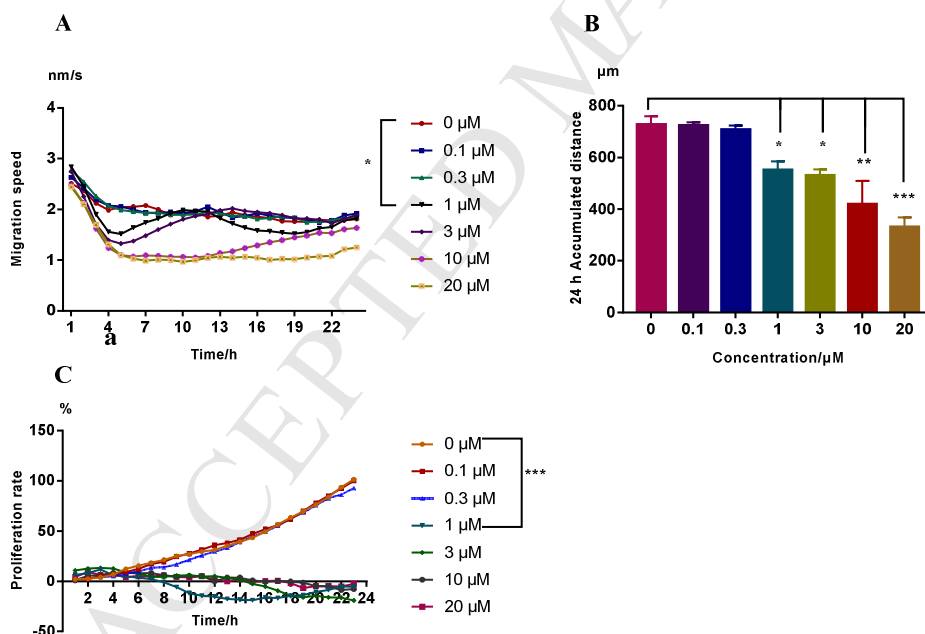


Fig. 7. (A) The migration speed of A375 cells after treatment with **6f**; (B) The accumulated distance of A375 cells after treatment with **6f**; (C) Proliferation rates. *, $P < 0.05$; **, $P < 0.01$; ***, $P < 0.001$.

4. Experimental section

4.1. General

Unless otherwise stated, the chemical starting materials were purchased from J&K, TCI, Innochem, Ark or Arcos and used without purification. The metal-catalysts were purchased from J&K, and solvents were used without pre-purification. All of the reactions were monitored by thin layer chromatography (TLC) on GF254 silica gel plates. Melting points were determined on X4 microscope and measured as uncorrected values. ^1H NMR and ^{13}C NMR spectra were recorded on Bruker AVANCE III 400 MHz and 100 MHz spectrometer respectively in CDCl_3 or $\text{DMSO-}d_6$. NMR chemical shifts are reported as values (ppm) relative to internal tetramethylsilane and splitting patterns are designated as: s = singlet, d = doublet, t = triplet, q = quartet, m = multiplet. HRMS of the products were carried out on Bruker Apex IV FTMS (Sample (about 0.1 mg) was dissolved in appropriate solvents (CH_3CN or MeOH) and detected the positive cationic signal.).

Cell Lines and Culture: H1299, HCT116 and A375 were purchased from ATCC. All the cell lines were maintained in appropriate medium as the manufacturer suggested. HCT116 and A375 were cultured in DMEM (H1299, RPMI 1640) medium (Sigma-Aldrich) supplemented with 10% fetal bovine serum (Gibco BRL, USA), in a humidified incubator at 37 °C and 5% CO_2 /95% air.

4.2. General procedure for the synthesis of compounds **6a-6o** and **15a-15c**

A solution of heteroaryl ketones (5.0 mmol), paraformaldehyde (10.0 mmol) with diisopropylammonium trifluoroacetate (5.0 mmol) in DMF (15 mL) was heated to 90 °C for 24 h. After the completion of the reaction monitored by TLC (PE/EA = 8/1), the reaction mixture was cooled down to room temperature and water (40 mL) was added. The mixture was then extracted with EtOAc (20 mL \times 3), and washed with saturated NaCl (aq) for three times. The organic phase was dried with anhydride sodium sulfate and concentrated under reduced vacuum. The crude product (**9a-9o**, **17a-17c**) was directly used in next step without further purification.

To a solution of pyridin-3-ylmethanamine (5.0 mmol) in DMF (15 mL) was added Et_3N (5.1 mmol, 0.71 mL) and CS_2 (5.0 mmol, 0.30 mL). The reaction mixture was

continuously stirred for 15 min, then the crude intermediate from **9a-9o** (or **17a-17c**) were added respectively, and the resulting mixture was stirred for 12 h at room temperature. Water (50 mL) was added and the mixture was extracted with ethyl acetate (15 mL×3). The combined organic phase was washed with saturated NaCl (aq) for three times, dried over anhydride sodium sulfate and concentrated under reduced vacuum. The residue was further purified by column chromatography on silica gel using PE/EA as eluent to afford **6a-6o** and **15a-15c**. Further recrystallized from hot EtOAc/PET to give crystals of the target compounds.

4.2.1.

*3-(1-Methyl-1H-pyrrolo[2,3-b]pyridin-3-yl)-3-oxopropyl
(pyridin-3-ylmethyl)carbamodithioate (6a)*

White solid, m. p. 150.9-151.8°C, yield: 47%, two steps. ¹H NMR (400 MHz, DMSO-*d*₆) δ 10.47 (t, *J* = 5.5 Hz, 1H), 8.57 (s, 1H), 8.54 – 8.41 (m, 3H), 8.38 (dd, *J* = 4.7, 1.4 Hz, 1H), 7.69 (d, *J* = 7.8 Hz, 1H), 7.36 (dd, *J* = 7.7, 4.9 Hz, 1H), 7.30 (dd, *J* = 7.8, 4.7 Hz, 1H), 4.85 (d, *J* = 5.6 Hz, 2H), 3.87 (s, 3H), 3.54 (t, *J* = 6.8 Hz, 2H), 3.29 (t, *J* = 6.9 Hz, 2H). ¹³C NMR (100 MHz, DMSO-*d*₆) δ 197.4, 192.6, 149.1, 148.4, 148.0, 144.1, 137.8, 135.5, 133.0, 129.7, 123.5, 118.4, 117.9, 113.2, 47.1, 38.2, 31.5, 29.2. HRMS *m/z* (ESI) calcd for C₁₈H₁₉N₄OS₂ (M+H)⁺: 371.0995, found 371.1004.

4.2.2.

*3-(1-Cyclobutyl-1H-pyrrolo[2,3-b]pyridin-3-yl)-3-oxopropyl
l(pyridin-3-ylmethyl)carbamodithioate (6b)*

White solid, m. p. 141.3-142.4°C, yield: 32%, two steps. ¹H NMR (400 MHz, DMSO-*d*₆) δ 10.50 (t, *J* = 5.5 Hz, 1H), 8.84 (s, 1H), 8.53 (d, *J* = 1.6 Hz, 1H), 8.51 – 8.43 (m, 2H), 8.36 (dd, *J* = 4.7, 1.5 Hz, 1H), 7.70 (d, *J* = 7.8 Hz, 1H), 7.37 (dd, *J* = 7.7, 4.8 Hz, 1H), 7.29 (dd, *J* = 7.8, 4.7 Hz, 1H), 5.33 (p, *J* = 8.8 Hz, 1H), 4.87 (d, *J* = 5.5 Hz, 2H), 3.57 (t, *J* = 6.8 Hz, 2H), 3.36 (t, *J* = 6.8 Hz, 2H), 2.86 – 2.55 (m, 2H), 2.46 (dd, *J* = 6.8, 3.5 Hz, 2H), 2.13 – 1.65 (m, 2H). ¹³C NMR (100 MHz, DMSO-*d*₆) δ 198.0, 193.4, 149.6, 148.9, 147.9, 144.4, 136.0, 135.1, 133.4, 130.4, 124.0, 119.1,

118.7, 114.3, 48.7, 47.6, 38.9, 30.6, 29.7, 15.0. HRMS m/z (ESI) calcd for $C_{21}H_{23}N_4OS_2$ (M+H)⁺: 411.1308, found 411.1311.

4.2.3.

*3-(1-Cyclopropyl-1H-pyrrolo[2,3-b]pyridin-3-yl)-3-oxopropyl
(pyridin-3-ylmethyl)carbamodithioate (6c)*

White solid, m. p. 147.7-149.1 °C, yield: 49%, two steps. ¹H NMR (400 MHz, DMSO-*d*₆) δ 10.49 (t, J = 5.5 Hz, 1H), 8.52 (d, J = 1.7 Hz, 1H), 8.50 (s, 1H), 8.49 – 8.43 (m, 2H), 8.38 (dd, J = 4.7, 1.6 Hz, 1H), 7.69 (dd, J = 6.0, 1.8 Hz, 1H), 7.36 (dd, J = 7.8, 4.8 Hz, 1H), 7.30 (dd, J = 7.9, 4.7 Hz, 1H), 4.86 (d, J = 5.6 Hz, 2H), 3.73 (dq, J = 7.4, 4.1 Hz, 1H), 3.55 (dd, J = 12.9, 5.9 Hz, 2H), 3.30 (t, J = 6.9 Hz, 2H), 1.34 – 0.87 (m, 4H). ¹³C NMR (100 MHz, DMSO-*d*₆) δ 197.5, 192.9, 149.1, 148.9, 148.4, 144.2, 136.0, 135.5, 133.0, 129.8, 123.5, 118.8, 118.5, 113.2, 47.1, 38.3, 29.3, 27.3, 6.1. HRMS m/z (ESI) calcd for $C_{20}H_{21}N_4OS_2$ (M+H)⁺: 397.1151, found 397.1159.

4.2.4.

*3-Oxo-3-(1-phenyl-1H-pyrrolo[2,3-b]pyridin-3-yl)propyl
(pyridin-3-ylmethyl)carbamodithioate (6d)*

White solid, m. p. 119.1-121.1 °C, yield: 54%, two steps. ¹H NMR (400 MHz, CDCl₃) δ 8.93 (s, 1H), 8.62 (d, J = 7.8 Hz, 1H), 8.43 (m, 3H), 8.24 (s, 1H), 7.72 (d, J = 7.8 Hz, 2H), 7.64 (d, J = 7.6 Hz, 1H), 7.54 (t, J = 7.7 Hz, 2H), 7.41 (t, J = 7.4 Hz, 1H), 7.27 – 7.22 (m, 1H), 7.22 – 7.09 (m, 1H), 4.90 (d, J = 5.1 Hz, 2H), 3.66 (t, J = 6.4 Hz, 2H), 3.40 (t, J = 6.5 Hz, 2H). ¹³C NMR (100 MHz, CDCl₃) δ 198.8, 193.7, 149.3, 148.9, 148.1, 145.2, 137.1, 136.2, 134.5, 132.5, 131.2, 129.7, 127.9, 124.6, 123.7, 119.4, 119.3, 115.9, 48.1, 39.6, 29.9. HRMS m/z (ESI) calcd for $C_{23}H_{21}N_4OS_2$ (M+H)⁺: 433.1151, found 433.1155.

4.2.5.

*3-Oxo-3-(1-(thiophen-2-yl)-1H-pyrrolo[2,3-b]pyridin-3-yl)propyl (pyridin-3-ylmethyl)
carbamodithioate (6e)*

Light yellow solid, m. p. 157.2-158.5°C, yield: 22%, two steps. ^1H NMR (400 MHz, DMSO- d_6) δ 10.51 (t, $J = 5.4$ Hz, 1H), 8.53 (s, 1H), 8.47 (t, $J = 3.6$ Hz, 2H), 8.25 (d, $J = 3.8$ Hz, 1H), 8.13 (d, $J = 7.7$ Hz, 1H), 7.94 (d, $J = 4.3$ Hz, 1H), 7.70 (d, $J = 7.8$ Hz, 1H), 7.60 (d, $J = 4.3$ Hz, 1H), 7.36 (dd, $J = 7.7, 4.8$ Hz, 1H), 7.30 (dd, $J = 7.8, 4.8$ Hz, 1H), 6.86 (d, $J = 3.8$ Hz, 1H), 4.86 (d, $J = 5.5$ Hz, 2H), 3.54 (t, $J = 6.7$ Hz, 2H), 3.47 – 3.29 (m, 2H). ^{13}C NMR (100 MHz, DMSO- d_6) δ 197.2, 191.2, 149.1, 148.4, 146.5, 145.9, 143.7, 135.6, 135.5, 132.9, 132.8, 129.9, 127.2, 123.5, 121.5, 118.0, 114.8, 104.6, 47.1, 37.7, 29.1. HRMS m/z (ESI) calcd for $\text{C}_{21}\text{H}_{19}\text{N}_4\text{OS}_3$ ($\text{M}+\text{H}$) $^+$: 439.0716, found 439.0721.

4.2.6.

3-(1-(2,2-Difluoroethyl)-1H-pyrrolo[2,3-b]pyridin-3-yl)-3-oxopropyl (pyridin-3-ylmethyl)carbamodithioate (6f)

White solid, m. p. 135.3-136.6°C, yield: 43%, two steps. ^1H NMR (400 MHz, DMSO- d_6) δ 10.49 (t, $J = 5.3$ Hz, 1H), 8.60 (s, 1H), 8.49 (dd, $J = 14.1, 6.7$ Hz, 3H), 8.41 (d, $J = 4.6$ Hz, 1H), 7.70 (d, $J = 7.7$ Hz, 1H), 7.49 – 7.28 (m, 2H), 6.51 (m, 1H), 5.00 – 4.74 (m, 4H), 3.56 (t, $J = 6.7$ Hz, 2H), 3.35 (d, $J = 3.8$ Hz, 2H). ^{13}C NMR (100 MHz, DMSO- d_6) δ 197.4, 192.9, 149.1, 148.4, 147.9, 144.5, 137.1, 135.5, 132.9, 130.1, 123.5, 118.9, 117.6, 114.4, 113.7, 47.1, 45.8 (t, $J_{\text{C-F}} = 26$ Hz), 38.5, 29.0. HRMS m/z (ESI) calcd for $\text{C}_{19}\text{H}_{19}\text{F}_2\text{N}_4\text{OS}_2$ ($\text{M}+\text{H}$) $^+$: 421.0963, found 421.0965.

4.2.7.

3-(4-Chloro-1H-pyrrolo[2,3-b]pyridin-3-yl)-3-oxopropyl (pyridin-3-ylmethyl)carbamodithioate (6g)

White solid, m. p. 158.9-160.0°C, yield: 26%, two steps. ^1H NMR (400 MHz, DMSO- d_6) δ 12.84 (s, 1H), 10.55 (d, $J = 45.4$ Hz, 1H), 8.59 (s, 1H), 8.52 (s, 1H), 8.47 (d, $J = 3.1$ Hz, 1H), 8.24 (d, $J = 4.4$ Hz, 1H), 7.69 (d, $J = 7.4$ Hz, 1H), 7.43 – 7.33 (m, 1H), 7.30 (d, $J = 5.1$ Hz, 1H), 4.85 (d, $J = 3.7$ Hz, 2H), 3.53 (t, $J = 6.0$ Hz, 2H), 3.47 – 3.29 (m, 2H). ^{13}C NMR (100 MHz, DMSO- d_6) δ 197.6, 191.4, 150.5, 149.1, 148.5, 144.7, 136.0, 135.9, 135.5, 133.0, 123.6, 119.3, 115.4, 115.3, 47.1, 39.4, 29.4. HRMS

m/z (ESI) calcd for C₁₇H₁₆ClN₄OS₂ (M+H)⁺: 391.0449, found 391.0450.

4.2.8.

*3-(4-Bromo-1H-pyrrolo[2,3-b]pyridin-3-yl)-3-oxopropyl
(pyridin-3-ylmethyl)carbamodithioate (6h)*

White solid, m. p. 165.7-167.0 °C, yield: 30%, two steps. ¹H NMR (400 MHz, DMSO-*d*₆) δ 12.79 (s, 1H), 10.47 (s, 1H), 8.51 (m, 3H), 8.14 (d, *J* = 5.0 Hz, 1H), 7.69 (d, *J* = 7.6 Hz, 1H), 7.48 (d, *J* = 5.0 Hz, 1H), 7.36 (dd, *J* = 7.3, 4.9 Hz, 1H), 4.86 (d, *J* = 5.3 Hz, 2H), 3.53 (t, *J* = 6.6 Hz, 2H), 3.34 (t, *J* = 6.6 Hz, 2H). ¹³C NMR (100 MHz, DMSO-*d*₆) δ 197.6, 191.5, 150.0, 149.1, 148.4, 144.3, 135.7, 135.5, 133.0, 124.5, 123.5, 122.9, 117.5, 115.4, 47.1, 39.7, 29.4. HRMS m/z (ESI) calcd for C₁₇H₁₆BrN₄OS₂ (M+H)⁺: 434.9943, found 434.9948.

4.2.9.

*3-(4-Cyclopropyl-1H-pyrrolo[2,3-b]pyridin-3-yl)-3-oxopropyl (pyridin-3-ylmethyl)
carbamodithioate (6i)*

White solid, m. p. 177.5-178.2 °C, yield: 18%, two steps. ¹H NMR (400 MHz, DMSO-*d*₆) δ 12.47 (s, 1H), 10.46 (t, *J* = 5.2 Hz, 1H), 8.52 (s, 2H), 8.47 (d, *J* = 4.4 Hz, 1H), 8.13 (d, *J* = 5.0 Hz, 1H), 7.69 (d, *J* = 7.7 Hz, 1H), 7.36 (dd, *J* = 7.6, 4.8 Hz, 1H), 6.59 (d, *J* = 5.1 Hz, 1H), 4.86 (d, *J* = 5.4 Hz, 2H), 3.63 (dd, *J* = 8.8, 3.9 Hz, 1H), 3.54 (t, *J* = 6.6 Hz, 2H), 3.38 (t, *J* = 6.7 Hz, 2H), 1.08 (d, *J* = 8.0 Hz, 2H), 0.81 (d, *J* = 4.4 Hz, 2H). ¹³C NMR (100 MHz, DMSO-*d*₆) δ 197.7, 192.6, 149.4, 149.1, 148.7, 148.4, 144.5, 135.9, 135.4, 132.9, 123.5, 116.8, 116.4, 111.3, 47.0, 38.9, 29.8, 13.1, 11.4. HRMS m/z (ESI) calcd for C₂₀H₂₁N₄OS₂ (M+H)⁺: 397.1151, found 397.1158.

4.2.10.

*3-(4-Ethynyl-1H-pyrrolo[2,3-b]pyridin-3-yl)-3-oxopropyl
(pyridin-3-ylmethyl)carbamodithioate (6j)*

White solid, m. p. 186.1-188.8 °C, yield: 20%, two steps. ¹H NMR (400 MHz, DMSO-*d*₆) δ 12.71 (s, 1H), 10.49 (s, 1H), 8.86 – 8.42 (m, 3H), 8.28 (s, 1H), 7.70 (s,

1H), 7.33 (d, $J = 24.5$ Hz, 2H), 4.85 (s, 2H), 4.59 (s, 1H), 3.52 (s, 2H), 3.35 (s, 2H). ^{13}C NMR (100 MHz, DMSO- d_6) δ 197.6, 191.5, 149.7, 149.1, 148.4, 143.7, 135.5, 133.0, 123.5, 123.3, 122.8, 116.1, 115.7, 109.5, 88.4, 82.0, 47.1, 39.0, 29.3. HRMS m/z (ESI) calcd for $\text{C}_{19}\text{H}_{17}\text{N}_4\text{OS}_2$ ($\text{M}+\text{H}$) $^+$: 381.0838, found 381.0838.

4.2.11.

3-Oxo-3-(4-phenyl-1H-pyrrolo[2,3-b]pyridin-3-yl)propyl

(pyridin-3-ylmethyl)carbamidithioate (6k)

White solid, m. p. 204.5-205.7°C, yield: 30%, two steps. ^1H NMR (400 MHz, DMSO- d_6) δ 12.63 (s, 1H), 10.46 (t, $J = 5.2$ Hz, 1H), 8.50 (d, $J = 11.8$ Hz, 3H), 8.36 (d, $J = 4.6$ Hz, 1H), 7.68 (d, $J = 7.4$ Hz, 1H), 7.35 (dt, $J = 11.4, 6.5$ Hz, 6H), 7.15 (d, $J = 4.8$ Hz, 1H), 4.84 (d, $J = 5.3$ Hz, 2H), 3.36 (s, 2H), 3.17 (t, $J = 6.7$ Hz, 2H). ^{13}C NMR (100 MHz, DMSO- d_6) δ 197.6, 191.5, 150.1, 149.1, 148.4, 144.1, 143.7, 140.0, 135.5, 134.6, 133.0, 128.5, 127.5, 123.5, 119.1, 116.5, 114.0, 47.1, 39.2, 29.7. HRMS m/z (ESI) calcd for $\text{C}_{23}\text{H}_{21}\text{N}_4\text{OS}_2$ ($\text{M}+\text{H}$) $^+$: 433.1151, found 433.1164.

4.2.12.

3-(5-Chloro-1H-pyrrolo[2,3-b]pyridin-3-yl)-3-oxopropyl

(pyridin-3-ylmethyl)carbamidithioate (6l)

White solid, m. p. 162.7-163.8°C, yield: 31%, two steps. ^1H NMR (400 MHz, DMSO- d_6) δ 12.75 (s, 1H), 10.47 (s, 1H), 8.59 (s, 1H), 8.52 (s, 1H), 8.47 (d, $J = 4.3$ Hz, 1H), 8.43 (s, 1H), 8.33 (s, 1H), 7.69 (d, $J = 7.5$ Hz, 1H), 7.56 – 7.24 (m, 1H), 4.85 (s, 2H), 3.54 (t, $J = 6.5$ Hz, 2H), 3.32 (t, $J = 6.5$ Hz, 2H). ^{13}C NMR (100 MHz, DMSO- d_6) δ 197.4, 193.2, 149.1, 148.4, 147.2, 142.5, 136.1, 135.5, 133.0, 128.4, 125.1, 123.5, 118.5, 114.2, 47.1, 38.3, 29.2. HRMS m/z (ESI) calcd for $\text{C}_{17}\text{H}_{16}\text{ClN}_4\text{OS}_2$ ($\text{M}+\text{H}$) $^+$: 391.0449, found 391.0456.

4.2.13.

3-(5-(4-Chlorophenyl)-1H-pyrrolo[2,3-b]pyridin-3-yl)-3-oxopropyl

(pyridin-3-ylmethyl)carbamidithioate (6m)

White solid, m. p. 182.9-184.7°C, yield: 24%, two steps. ^1H NMR (400 MHz, DMSO- d_6) δ 12.65 (s, 1H), 10.48 (s, 1H), 8.64 (dd, $J = 14.6, 2.2$ Hz, 2H), 8.60 – 8.41 (m, 3H), 7.75 (d, $J = 8.5$ Hz, 2H), 7.69 (d, $J = 7.8$ Hz, 1H), 7.55 (d, $J = 8.5$ Hz, 2H), 7.36 (dd, $J = 7.7, 4.8$ Hz, 1H), 4.86 (d, $J = 5.5$ Hz, 2H), 3.56 (s, 2H), 3.35 (d, $J = 6.8$ Hz, 2H). ^{13}C NMR (100 MHz, DMSO- d_6) δ 197.5, 193.3, 149.1, 148.6, 148.4, 143.2, 137.3, 135.5, 135.4, 133.0, 132.3, 129.5, 129.1, 128.8, 127.3, 123.5, 117.7, 114.8, 47.1, 38.3, 29.3. HRMS m/z (ESI) calcd for $\text{C}_{23}\text{H}_{20}\text{ClN}_4\text{OS}_2$ (M+H) $^+$: 467.0762, found 467.0772.

4.2.14.

*3-(6-Chloro-1H-pyrrolo[2,3-b]pyridin-3-yl)-3-oxopropyl
(pyridin-3-ylmethyl)carbamodithioate (6n)*

White solid, m. p. 180.6-182.6°C, yield: 21%, two steps. ^1H NMR (400 MHz, DMSO- d_6) δ 12.71 (s, 1H), 10.47 (t, $J = 5.3$ Hz, 1H), 8.57 – 8.50 (m, 2H), 8.47 (d, $J = 7.9$ Hz, 2H), 7.69 (d, $J = 7.8$ Hz, 1H), 7.46 – 7.24 (m, 2H), 4.85 (d, $J = 5.4$ Hz, 2H), 3.54 (t, $J = 6.7$ Hz, 2H), 3.32 (t, $J = 6.7$ Hz, 2H). ^{13}C NMR (100 MHz, DMSO- d_6) δ 197.4, 193.2, 149.1, 148.4, 147.8, 144.4, 135.5, 134.8, 132.9, 132.6, 123.5, 118.0, 116.5, 114.8, 47.1, 38.3, 29.1. HRMS m/z (ESI) calcd for $\text{C}_{17}\text{H}_{16}\text{ClN}_4\text{OS}_2$ (M+H) $^+$: 391.0449, found 391.0457.

4.2.15.

*3-(6-Methyl-1H-pyrrolo[2,3-b]pyridin-3-yl)-3-oxopropyl
(pyridin-3-ylmethyl)carbamodithioate (6o)*

White solid, m. p. 174.4-176.2°C, yield: 22%, two steps. ^1H NMR (400 MHz, DMSO- d_6) δ 12.31 (s, 1H), 10.46 (t, $J = 5.5$ Hz, 1H), 8.52 (d, $J = 1.6$ Hz, 1H), 8.47 (dd, $J = 4.7, 1.4$ Hz, 1H), 8.38 (d, $J = 3.1$ Hz, 1H), 8.33 (d, $J = 8.0$ Hz, 1H), 7.69 (d, $J = 7.8$ Hz, 1H), 7.36 (dd, $J = 7.7, 4.7$ Hz, 1H), 7.12 (d, $J = 8.0$ Hz, 1H), 4.85 (d, $J = 5.6$ Hz, 2H), 3.53 (t, $J = 6.8$ Hz, 2H), 3.28 (t, $J = 6.8$ Hz, 2H), 2.53 (s, 3H). ^{13}C NMR (100 MHz, DMSO- d_6) δ 197.5, 193.1, 152.8, 149.1, 148.7, 148.4, 135.5, 133.5, 133.0, 129.7, 123.5, 117.9, 115.1, 114.7, 47.1, 38.1, 29.3, 24.0. HRMS m/z (ESI) calcd for

$C_{18}H_{19}N_4OS_2$ (M+H)⁺: 371.0995, found 371.1002.

4.2.16.

3-Oxo-3-(pyrazolo[1,5-a]pyridin-3-yl)propyl (pyridin-3-ylmethyl)carbamodithioate (15a)

White solid, m. p. 144.0-145.3 °C, yield: 52%, two steps. ¹H NMR (400 MHz, DMSO-*d*₆) δ 10.48 (t, *J* = 5.2 Hz, 1H), 8.87 (d, *J* = 6.8 Hz, 1H), 8.69 (s, 1H), 8.52 (s, 1H), 8.47 (d, *J* = 3.9 Hz, 1H), 8.23 (d, *J* = 8.8 Hz, 1H), 7.79 – 7.56 (m, 2H), 7.35 (dd, *J* = 7.6, 4.9 Hz, 1H), 7.19 (t, *J* = 6.6 Hz, 1H), 4.86 (d, *J* = 5.4 Hz, 2H), 3.55 (t, *J* = 6.7 Hz, 2H), 3.34 (t, *J* = 6.9 Hz, 2H). ¹³C NMR (100 MHz, DMSO-*d*₆) δ 197.4, 191.6, 149.1, 148.4, 145.0, 139.3, 135.4, 132.9, 129.9, 129.4, 123.5, 118.7, 115.1, 111.6, 47.1, 39.2, 29.1. HRMS *m/z* (ESI) calcd for $C_{17}H_{17}N_4OS_2$ (M+H)⁺: 357.0838, found 357.0848.

4.2.17.

3-Oxo-3-(pyrazolo[1,5-b]pyridazin-3-yl)propyl (pyridin-3-ylmethyl)carbamodithioate (15b)

White solid, m. p. 160.0-160.9 °C, yield: 18%, two steps. ¹H NMR (400 MHz, DMSO-*d*₆) δ 10.50 (d, *J* = 5.4 Hz, 1H), 8.81 (s, 1H), 8.68 (ddd, *J* = 10.6, 6.7, 1.6 Hz, 2H), 8.52 (s, 1H), 8.47 (d, *J* = 4.6 Hz, 1H), 7.69 (d, *J* = 7.8 Hz, 1H), 7.58 (dd, *J* = 9.0, 4.5 Hz, 1H), 7.37 (dd, *J* = 7.8, 4.8 Hz, 1H), 4.85 (d, *J* = 5.5 Hz, 2H), 3.55 (t, *J* = 6.7 Hz, 2H), 3.40 (t, *J* = 6.7 Hz, 2H). ¹³C NMR (100 MHz, DMSO-*d*₆) δ 197.3, 192.4, 149.1, 148.4, 144.9, 142.4, 135.5, 133.8, 132.9, 128.3, 123.5, 121.4, 111.8, 47.1, 39.4, 28.7. HRMS *m/z* (ESI) calcd for $C_{16}H_{16}N_5OS_2$ (M+H)⁺: 358.0791, found 358.0801.

4.2.18.

3-Oxo-3-(2-phenylpyrazolo[1,5-b]pyridazin-3-yl)propyl (pyridin-3-ylmethyl)carbamodithioate (15c)

White solid, m. p. 160.2-161.0 °C, yield: 30%, two steps. ¹H NMR (400 MHz, DMSO-*d*₆) δ 10.55 (s, 1H), 8.69 (dd, *J* = 16.0, 6.6 Hz, 2H), 8.57 – 8.30 (m, 2H), 7.79

– 7.56 (m, 4H), 7.56 – 7.43 (m, 3H), 7.40 – 7.27 (m, 1H), 4.79 (d, $J = 5.4$ Hz, 2H), 3.38 (t, $J = 6.2$ Hz, 2H), 2.94 (t, $J = 6.5$ Hz, 2H). ^{13}C NMR (100 MHz, DMSO- d_6) δ 197.0, 193.3, 153.0, 149.1, 148.4, 145.0, 135.6, 135.5, 133.0, 132.5, 129.8, 129.3, 128.6, 128.4, 123.5, 121.3, 110.1, 47.0, 41.3, 28.7. HRMS m/z (ESI) calcd for $\text{C}_{22}\text{H}_{20}\text{N}_5\text{OS}_2$ ($\text{M}+\text{H}$) $^+$: 434.1104, found 434.1112.

4.3. Synthesis of 7-azaindole derivatives

4.3.1. General procedure for the synthesis of compounds **8g**, **8h** and **8l**

7-Azaindole derivatives (4.2 mmol) were added to a stirred suspension of AlCl_3 (21.0 mmol, 2.80 g) in DCM (40 mL) placed at ice bath. After the mixture was stirred at room temperature for 0.5 h, acetyl chloride (21.0 mmol, 1.49 mL) was added dropwise and the resulting mixture was reacted for 12 h at room temperature. MeOH (20 mL) was added cautiously to quench the reaction, the solvents were removed under reduced vacuum. Then the residue was dissolved in 40 mL water, 1N NaOH (aq) was added to adjust the pH up to 5, and extracted with ethyl acetate (15 mL \times 3). The combined organic phase was dried over anhydride sodium sulfate and concentrated under reduced vacuum. The residue was further purified by column chromatography on silica gel using PE/EA as eluent to afford the corresponding acylated product.

1-(4-Chloro-1H-pyrrolo[2,3-b]pyridin-3-yl)ethenone (**8g**) [53]. White solid, yield: 50%. ^1H NMR (400 MHz, DMSO- d_6) δ 12.79 (s, 1H), 8.56 (s, 1H), 8.23 (d, $J = 5.1$ Hz, 1H), 7.29 (d, $J = 5.0$ Hz, 1H), 2.50 (s, 3H).

1-(4-Bromo-1H-pyrrolo[2,3-b]pyridin-3-yl)ethenone (**8h**) [53]. White solid, yield: 52%. ^1H NMR (400 MHz, DMSO- d_6) δ 12.77 (s, 1H), 8.56 (s, 1H), 8.13 (d, $J = 5.1$ Hz, 1H), 7.47 (d, $J = 5.0$ Hz, 1H), 2.50 (s, 3H).

1-(5-Chloro-1H-pyrrolo[2,3-b]pyridin-3-yl)ethenone (**8l**) [53]. White solid, yield: 88%. ^1H NMR (400 MHz, CDCl_3) δ 10.63 (s, 1H), 8.70 (s, 1H), 8.36 (s, 1H), 8.01 (s,

1H), 2.55 (s, 3H).

4.3.2. Synthesis of compounds **8a**, **8b** and **8f**

To a solution of 7-azaindole (4.0 mmol, 472 mg) in anhydrous THF (10 mL) was added 60% NaH (8.2 mmol, 328 mg) placed at ice bath, 30 minutes later, dimethyl sulfate (0.4 mL) was added dropwise to the solution. The resulting mixture was continuously stirred at room temperature for 10 hours. Water (30 mL) was added cautiously to quench the reaction, and the solution was extracted with EtOAc (10 mL×3). The combined organic phase was washed with saturated NaCl (aq) for three times, dried over anhydride sodium sulfate and concentrated under reduced vacuum. The residue was further purified by column chromatography on silica gel using PE/EA as eluent to afford **7a** (yield: 95%).

Following the procedure 4.3.1, using **7a** as the starting material, compound **8a** was obtained as a white solid, yield 75%. 1-(1-Methyl-1H-pyrrolo[2,3-b]pyridin-3-yl)ethenone (**8a**) [54]. ¹H NMR (400 MHz, CDCl₃) δ 8.61 (dd, *J* = 7.9, 1.5 Hz, 1H), 8.40 (dd, *J* = 4.7, 1.5 Hz, 1H), 7.84 (s, 1H), 7.27 – 7.18 (m, 1H), 3.94 (s, 3H), 2.52 (s, 3H); ¹³C NMR (100 MHz, CDCl₃) δ 192.8, 148.3, 144.5, 135.4, 130.9, 118.7, 118.5, 115.3, 31.9, 27.2.

To a solution of 7-azaindole (5.0 mmol, 0.590 mg) in DMF (15 mL) was added Cs₂CO₃ (10.0 mmol, 3.26 g) and bromocyclobutane (7.5 mmol, 1.00 g). The mixture was heated to 90°C and reacted for 20 hours. After the completion of the reaction monitored by TLC (PE/EA = 10/1), the reaction mixture was cooled down to room temperature and water (40 mL) was added. The mixture was then extracted with EtOAc (15 mL×3), and washed with saturated NaCl (aq) for three times. The organic phase was dried with anhydride sodium sulfate and concentrated under reduced vacuum. The residue was further purified by column chromatography on silica gel using PE/EA as eluent to afford **7b** (yield: 89%).

Following the procedure 4.3.1, using **7b** as the starting material, compound **8b** was obtained as a white solid, yield 94%. 1-(1-Cyclobutyl-1H-pyrrolo[2,3-b]

pyridin-3-yl)ethenone (**8b**) [55]. ^1H NMR (400 MHz, CDCl_3) δ 8.59 (dd, $J = 7.9, 1.5$ Hz, 1H), 8.47 – 8.26 (m, 1H), 8.04 (s, 1H), 7.23 (dd, $J = 7.9, 4.7$ Hz, 1H), 5.61 – 5.09 (m, 1H), 2.77 – 2.59 (m, 2H), 2.56 (s, 3H), 2.49 (ddd, $J = 19.3, 9.8, 2.6$ Hz, 2H), 2.09 – 1.90 (m, 2H).

Following the above procedure for **7b**, using **5b** as the starting material, compound **8f** was obtained as a white solid, yield 88%. 1-(1-(2,2-Difluoroethyl)-1H-pyrrolo[2,3-b]pyridin-3-yl)ethenone. (**8f**) ^1H NMR (400 MHz, CDCl_3) δ 8.63 (dd, $J = 7.9, 1.4$ Hz, 1H), 8.38 (dd, $J = 4.7, 1.4$ Hz, 1H), 7.90 (s, 1H), 7.27 (dd, $J = 7.9, 4.7$ Hz, 1H), 6.18 (m, 1H), 4.69 (td, $J = 14.1, 4.1$ Hz, 2H), 2.53 (s, 3H). ESI m/z (ESI) calcd for $\text{C}_{11}\text{H}_{11}\text{F}_2\text{N}_2\text{O}$ ($\text{M}+\text{H}$) $^+$: 225.08, found 225.10.

4.3.3. Synthesis of compound **8c**

To a suspension of cyclopropylboronic acid (10.1 mmol, 872 mg), 7-azaindole (5.1 mmol, 590 mg), and Na_2CO_3 (10.1 mmol, 1.10 g) in 15 mL dichloroethane was added a suspension of $\text{Cu}(\text{OAc})_2$ (5.0 mmol, 922 mg) and bipyridine (5.0 mmol, 793 mg) in hot DCE (2.0 mL). The mixture was heated to reflux and stirred for 10 h under air. The resulting mixture was cooled to room temperature, and a saturated aqueous NH_4Cl solution was added, followed by water. The organic layer was separated, and the aqueous layer was extracted with DCM (15 mL \times 3) for three times. The organic phase was dried with anhydride sodium sulfate and concentrated under reduced vacuum. The residue was further purified by column chromatography on silica gel using PE/EA as eluent to afford **7c** (yield: 55%).

Following the procedure 4.3.1, using **7c** as the starting material, compound **8c** was obtained as a white solid, yield 44%. 1-(1-Cyclopropyl-1H-pyrrolo[2,3-b]pyridin-3-yl) ethenone (**8c**). ^1H NMR (400 MHz, CDCl_3) δ 8.77 – 8.51 (m, 1H), 8.44 (d, $J = 4.7$ Hz, 1H), 7.83 (s, 1H), 7.25 (dd, $J = 7.9, 4.7$ Hz, 1H), 3.63 (tt, $J = 7.4, 3.9$ Hz, 1H), 2.52 (s, 3H), 1.24 (q, $J = 7.0$ Hz, 2H), 1.19 – 1.03 (m, 2H). ESI m/z (ESI) calcd for $\text{C}_{11}\text{H}_{13}\text{N}_2\text{O}$ ($\text{M}+\text{H}$) $^+$: 201.10, found 201.10.

4.3.4. Synthesis of compounds **8d** and **8e**

Under argon, CuI (10 mol%, 96 mg) and ethylenediamine (20 mol%, 60 mg) were added to a solution of 7-azaindole (5.0 mmol, 590 mg), aryl halide (5.5 mmol) and potassium phosphate (10.0 mmol, 2.66 g) in 1,4-dioxane (15 mL). The mixture was heated to reflux and reacted for overnight. Then it was cooled down to room temperature, filtered, diluted with water (30 mL), and extracted with EtOAc (10 mL×3). The combined organic phase was dried with anhydride sodium sulfate and concentrated under reduced vacuum. The residue was further purified by column chromatography on silica gel using PE/EA as eluent to afford product (**7d**, yield: 90%; **7e**, yield: 75%).

Following the procedure 4.3.1, using **7d** as the starting material, compound **8d** was obtained as a white solid, yield 75%. 1-(1-Phenyl-1H-pyrrolo[2,3-b]pyridin-3-yl)ethenone (**8d**) [53, 56]. ¹H NMR (400 MHz, CDCl₃) δ 8.71 (dd, *J* = 7.9, 1.6 Hz, 1H), 8.43 (dd, *J* = 4.7, 1.6 Hz, 1H), 8.10 (s, 1H), 7.74 (dd, *J* = 8.4, 0.8 Hz, 2H), 7.57 (dd, *J* = 10.8, 5.0 Hz, 2H), 7.44 (t, *J* = 7.5 Hz, 1H), 7.30 (dd, *J* = 7.9, 4.7 Hz, 1H), 2.59 (s, 3H).

Following the procedure 4.3.1, using **7e** as the starting material, compound **8e** was obtained as a yellow solid, yield 53%. 1-(1-(Thiophen-2-yl)-1H-pyrrolo[2,3-b]pyridin-3-yl)ethenone (**8e**). ¹H NMR (400 MHz, CDCl₃) δ 8.44 (d, *J* = 4.5 Hz, 1H), 7.93 (d, *J* = 7.8 Hz, 1H), 7.62 (d, *J* = 3.8 Hz, 1H), 7.56 (d, *J* = 2.9 Hz, 1H), 7.42 (d, *J* = 3.8 Hz, 1H), 7.23 – 7.08 (m, 1H), 6.66 (d, *J* = 2.8 Hz, 1H), 2.55 (s, 3H). ESI *m/z* (ESI) calcd for C₁₃H₁₁N₂OS (M+H)⁺: 243.06, found 243.06.

4.3.5. Synthesis of compound **8i**

To a solution of 4-Br-7-azaindole (3.0 mmol, 600 mg), tetrabutylammonium hydrogen sulfate (3 mol%, 28 mg) and tosyl chloride (4.0 mmol, 736 mg) in DCM (15 mL) placed at ice bath was added 1N NaOH solutions (3.0 mL). The resulting mixture was stirred at room temperature for 2 hours. Water (30 mL) was added cautiously to the reaction, and the mixture was extracted with DCM (15 mL×3). The combined organic phase was washed with saturated NaCl (aq) for three times, dried over

anhydride sodium sulfate and concentrated under reduced vacuum. The crude product (**11a**) was directly used in next step.

Under argon, Pd(OAc)₂ (10 mol%, 67 mg) and X-phos (5 mol%, 71 mg) were added to a solution of **11a** (3.0 mmol, 1.04 g), Cs₂CO₃ (6.0 mmol, 1.95 g) and cyclopropylboronic acid (4.5 mmol, 390 mg) in toluene/H₂O mixed solutions (v/v, 15 mL/5 mL). The mixture was heated to reflux and reacted for 20 h. Then it was cooled down to room temperature, filtered through a layer of diatomaceous earth, diluted with water (30 mL), and extracted with EtOAc (15 mL×3). The organic phase was dried with anhydride sodium sulfate and concentrated under reduced vacuum. The residue was further purified by column chromatography on silica gel using PE/EA as eluent to afford product **11b**, yield: 68%.

To a solution of **11b** (2.37 mmol, 741 mg) in 15 mL ethanol was added 4N NaOH solutions (6.0 mL). The resulting mixture was heated to reflux for 4 hours, cooled down to room temperature and concentrated under reduced vacuum. Water (30 mL) was added to the reaction, and the mixture was extracted with EtOAc (10 mL×3). The combined organic phase was dried over anhydride sodium sulfate and concentrated under reduced vacuum. The residue was further purified by column chromatography on silica gel using PE/EA as eluent to afford product **7i**, yield: 87%.

Following the procedure 4.3.1, using **7i** as the starting material, compound **8i** was obtained as a white solid, yield 50%. 1-(4-Cyclopropyl-1H-pyrrolo[2,3-b]pyridin-3-yl)ethenone (**8i**) [53, 56]. ¹H NMR (400 MHz, DMSO-*d*₆) δ 12.44 (s, 1H), 8.49 (s, 1H), 8.12 (d, *J* = 5.1 Hz, 1H), 6.57 (d, *J* = 5.2 Hz, 1H), 3.67 (s, 1H), 2.52 (s, 3H), 1.06 (dt, *J* = 6.1, 4.1 Hz, 2H), 0.89 – 0.65 (m, 2H).

4.3.6. Synthesis of compound **8j**

4-Br-7-azaindole (4.0 mmol, 1.80 g), trimethylsilylacetylene (6.0 mmol, 590 mg) and Et₃N (15 mL) were placed in a round bottomed flask followed by the addition of CuI (6 mol%, 60 mg) and Pd(PPh₃)₂Cl₂ (3 mol%, 108 mg) under argon. The mixture

was heated to 45°C for overnight, filtered and concentrated under reduced vacuum. The crude product was dissolved in 15 mL MeOH, followed by the addition of 1N NaOH solutions (5 mL), stirred for 4 hours at room temperature and concentrated under reduced vacuum. Water (40 mL) was added to the reaction, and the mixture was extracted with EtOAc (10 mL×3). The combined organic phase was dried over anhydride sodium sulfate and concentrated under reduced vacuum. The residue was further purified by column chromatography on silica gel using PE/EA as eluent to afford product **7j**, yield: 72% (two steps).

Following the procedure 4.3.1, using **7j** as the starting material, compound **8j** was obtained as a light yellow solid, yield 70%. 1-(4-Ethynyl-1H-pyrrolo[2,3-b]pyridin-3-yl)ethenone (**8j**). ¹H NMR (400 MHz, DMSO-*d*₆) δ 12.65 (s, 1H), 8.50 (s, 1H), 8.27 (d, *J* = 4.9 Hz, 1H), 7.29 (d, *J* = 4.9 Hz, 1H), 4.57 (s, 1H), 2.49 (s, 3H). ESI *m/z* (ESI) calcd for C₁₁H₉N₂O (M+H)⁺: 185.07, found 185.08.

4.3.7. Synthesis of compounds **8k** and **8m**

Under argon, Pd(OAc)₂ (5 mol%, 45 mg) and dppf (5 mol%, 111 mg) were added to a solution of 4-Br-7-azaindole (4.0 mmol, 788 mg), Cs₂CO₃ (10.0 mmol, 3.25 g) and phenylboronic acid (8.0 mmol, 976 mg) in toluene/H₂O mixed solution (v/v, 15 mL/5 mL). The mixture was heated to reflux and reacted for overnight. Then the mixture was cooled down to room temperature, filtered through a layer of diatomaceous earth, diluted with water (30 mL), and extracted with EtOAc (15 mL×3). The organic phase was dried with anhydride sodium sulfate and concentrated under reduced vacuum. The residue was further purified by column chromatography on silica gel using PE/EA as eluent to afford product **7k**, yield: 75%.

Following the procedure 4.3.1, using **7k** as the starting material, compound **8k** was obtained as a white solid, yield 42%. 1-(4-Phenyl-1H-pyrrolo[2,3-b]pyridin-3-yl)ethenone (**8k**) [53]. ¹H NMR (400 MHz, DMSO-*d*₆) δ 12.59 (s, 1H), 8.46 (s, 1H), 8.35 (d, *J* = 4.9 Hz, 1H), 7.37 (d, *J* = 5.9 Hz, 3H), 7.31 (dd, *J* = 7.0, 2.2 Hz, 2H), 7.12 (d, *J* = 4.9 Hz, 1H), 2.29 (s, 3H).

Following the above procedure, using 5-Cl-7-azaindole and *p*-chlorobenzoic acid as the starting material, compound **8m** was obtained as a white solid, yield 42%. 1-(5-(4-Chlorophenyl)-1H-pyrrolo[2,3-b]pyridin-3-yl)ethanone (**8m**) [53]. ¹H NMR (400 MHz, DMSO-*d*₆) δ 12.60 (s, 1H), 8.63 (dd, *J* = 13.1, 2.2 Hz, 2H), 8.52 (s, 1H), 7.73 (d, *J* = 8.5 Hz, 2H), 7.53 (d, *J* = 8.5 Hz, 2H), 2.49 (s, 3H).

4.3.8. Synthesis of compounds **8n** and **8o**

To a solution of 7-azaindole (5.0 mmol, 590 mg) in 30 mL EtOAc was slowly added 70% *m*-CPBA (7.5 mmol, 1.30 g). The resulting mixture was reacted at room temperature for 2 hours, filtered, and got the intermediate 7-azaindole N-oxide **13a**, yield: quantify.

Under argon, **13a** (5.0 mmol), HMDS (6.0 mmol, 966 mg) and toluene (20 mL) were placed in a round bottomed flask followed by the addition of benzoyl chloride (6.0 mmol, 840 mg). After stirring for 2 hours at room temperature, the solvents were removed under reduced vacuum. The crude product **13b** was again dissolved in 15 mL methanol and 1N NaOH solutions (10 mL) were added dropwise. The reaction was stirred for overnight at room temperature, diluted with water (40 mL), and extracted with EtOAc (15 mL×3). The organic phase was dried with anhydride sodium sulfate and concentrated under reduced vacuum. The residue was further purified by column chromatography on silica gel using PE/EA as eluent to afford product **7n**, yield: 33% (two steps). 6-Chloro-1H-pyrrolo[2,3-b]pyridine (**7n**) [40]. ¹H NMR (400 MHz, CDCl₃) δ 11.21 (s, 1H), 7.91 (d, *J* = 8.2 Hz, 1H), 7.41 (dd, *J* = 3.3, 2.6 Hz, 1H), 7.11 (d, *J* = 8.2 Hz, 1H), 6.52 (dd, *J* = 3.4, 2.0 Hz, 1H).

Following the procedure 4.3.1, using **7n** as the starting material, compound **8n** was obtained as a yellow solid, yield 20%. 1-(6-Chloro-1H-pyrrolo[2,3-b]pyridin-3-yl)ethenone (**8n**) [41]. ¹H NMR (400 MHz, DMSO-*d*₆) δ 12.66 (s, 1H), 8.49 (s, 1H), 8.46 (d, *J* = 8.2 Hz, 1H), 7.30 (d, *J* = 8.2 Hz, 1H), 2.46 (s, 3H).

To a solution of **7n** (2.7 mmol, 410 mg), tetrabutylammonium hydrogen sulfate (3 mol%, 27 mg) and benzene sulfonyl chloride (3.3 mmol, 583 mg) in DCM (15 mL)

placed at ice bath was added 1N NaOH solutions (3.0 mL). The resulting mixture was stirred at room temperature for 8 hours. Water (30 mL) was added cautiously to the reaction, and the mixture was extracted with DCM (15 mL×3). The combined organic phase was washed with saturated NaCl (aq) for three times, dried over anhydride sodium sulfate and concentrated under reduced vacuum. The crude product (**14a**) was directly used in next step.

Under argon, Pd(PPh₃)₄ (0.13 mmol, 144 mg) and pre-prepared MeZnCl (18 mmol, dissolved in anhydrous THF) were added to a solution of **14a** (2.6 mmol, 716 mg) in anhydrous THF (10 mL). The mixture was heated to reflux and reacted for 48 h. Then the mixture was cooled down to room temperature, filtered through a layer of diatomaceous earth, diluted with water (40 mL), and extracted with EtOAc (15 mL×3). The organic phase was dried with anhydride sodium sulfate and concentrated under reduced vacuum. The residue was further purified by column chromatography on silica gel using PE/EA as eluent to afford product **14b**, yield: 68%.

To a solution of **14b** (4.50 mmol, 1.22 g) in 30 mL ethanol was added 4N NaOH solutions (10 mL). The resulting mixture was heated to reflux for 10 hours, cooled down to room temperature and concentrated under reduced vacuum. Water (30 mL) was added to the reaction, and the mixture was extracted with EtOAc (15 mL×3). The combined organic phase was dried over anhydride sodium sulfate and concentrated under reduced vacuum. The residue was further purified by column chromatography on silica gel using PE/EA as eluent to afford product **7o**, yield: 70%.

Following the procedure 4.3.1, using **7o** as the starting material, compound **8o** was obtained as a white solid, yield 30%. 1-(6-Methyl-1H-pyrrolo[2,3-b]pyridin-3-yl)ethenone (**8o**) [41]. ¹H NMR (400 MHz, DMSO-*d*₆) δ 12.29 (s, 1H), 8.33 (d, *J* = 8.2 Hz, 2H), 7.10 (d, *J* = 8.0 Hz, 1H), 2.53 (s, 3H), 2.44 (s, 3H).

4.4. Synthesis of acetylated heteroaryl cycles

4.4.1.

1-(Pyrazolo[1,5-a]pyridin-3-yl)ethenone (**16a**) [43]. Light yellow solid, yield: 52%.

^1H NMR (400 MHz, CDCl_3) δ 8.54 (d, $J = 6.9$ Hz, 1H), 8.40 (d, $J = 8.9$ Hz, 1H), 8.35 (s, 1H), 7.60 – 7.40 (m, 1H), 7.15 – 6.86 (m, 1H), 2.56 (s, 3H).

4.4.2.

1-(Pyrazolo[1,5-b]pyridazin-3-yl)ethanone (**16b**) [42]. Brown solid, yield 46%. ^1H NMR (400 MHz, CDCl_3) δ 8.75 (dd, $J = 9.0, 1.9$ Hz, 1H), 8.48 (dd, $J = 4.4, 1.9$ Hz, 1H), 8.44 (s, 1H), 7.33 (dd, $J = 9.0, 4.5$ Hz, 1H), 2.60 (s, 3H).

4.4.3.

1-(2-Phenylpyrazolo[1,5-b]pyridazin-3-yl)ethanone (**16c**) [42]. Brown solid, yield 44%. ^1H NMR (400 MHz, CDCl_3) δ 8.77 (d, $J = 9.0$ Hz, 1H), 8.48 (d, $J = 3.9$ Hz, 1H), 7.64 (s, 2H), 7.52 (d, $J = 2.7$ Hz, 3H), 7.33 (dd, $J = 9.0, 4.5$ Hz, 1H), 2.20 (s, 3H).

4.5. *Biological assay*

Pyruvate kinase activity was detected with a fluorescent pyruvate kinase-lactate dehydrogenase coupled assay described in the previous reference [39].

4.6. *Anti-proliferation activity assay*

Cell lines were cultured in RPMI 1640 (H1299) or DMEM (HCT116, A375) containing 10% fetal bovine serum (FBS) at 37°C in 5% CO_2 . Cell viability was detected with the Cell-Titer-Glo™ assay (Promega) according to the manufacturer's instructions. Briefly, 2000 cells in per well were plated in 384-well plates. After incubated for 24 h, the cells were treated with ten different concentration of tested compound or DMSO (as negative control) for 72 h. Then 20 μL CellTiter-Glo reagents were added to the well and incubated at room temperature for 30 mins kept in dark place. Record the luminescence by a microplate reader (Flexstation 3). The IC_{50} values were calculated using Graphpad Prism of the triplicate experiment.

4.7. *High content screening for immunostaining assay*

For nuclear translocation assay, A375 cells were seeded into special 96-well plate at 60% concentration per well and incubated at 37°C for 24 h. The cells were treated with three different concentrations of compound **6f**, DMSO (as negative control) and **NZT**, incubated at 37°C for another 24 h. Then the cells were washed with 500 μ L PBS once, fixed with 200 μ L of 3% PFA and 0.1% glutaraldehyde for 10 minutes at room temperature. After that, the cells were washed with 500 μ L PBS again for twice, and blocked by blocking buffer (200 μ L) at 4°C for overnight, which was further incubated with primary antibody dilutions in blocking buffer (100 μ L) for 2 hours at room temperature. The primary antibody dilutions (rabbit anti-PKM2) were then washed by washing buffer (200 μ L) for three times followed by the addition of secondary antibody dilutions (40 μ L) in blocking buffer and Hoechst 33258 (10 μ L) in blocking buffer for 1 hour at room temperature. When the secondary antibody dilutions were washed by washing buffer (100 μ L) for three times, it was ready for detecting the immunostaining in Operetta living cell workstations.

For autophagy assay, the primary antibody was replaced by rabbit anti-LC3B antibody.

Solutions:

1. Fixation solution: 3% paraformaldehyde (PFA) + 0.1% glutaraldehyde in PBS;
2. Blocking buffer: 3% BSA + 0.2% Triton™ X-100 in PBS;
3. Washing buffer: 0.2% BSA + 0.05% Triton™ X-100 in PBS;

4.8. Apoptosis detected by Annexin V and PI staining

For cell apoptosis assay, A375 cells were seeded into a six-well plate at 6×10^5 cells per well. After 24 h, the cultured medium was replaced with fresh medium containing different concentrations of compound **6f** for another 24 h incubation. Then the cells were harvested by trypsinization, washed twice with ice-cold PBS and stained with the AnnexinV-FITC/PI apoptosis kit (KeyGEN BioTECH, USA) according to the manufacturer's instructions. Cells in early apoptosis was stained with Annexin V alone (Annexin V⁺/PI), whereas those in the advanced stages of apoptosis was stained with both Annexin V and PI (Annexin V⁺/PI⁺). On the contrary, the Annexin V and PI

double-negative (Annexin V⁻/PI⁻) cells were considered alive.

4.9. Migration and proliferation rate assay

A375 cell lines were seeded into a special 96-well plate at 60% cells per well. After incubated for 24 h, the cells were treated with six different concentration of tested compound or DMSO (as negative control). The migration distance or proliferation rate could be monitored in real time using the high content software Operetta. The depicted data were calculated using Graphpad Prism of the triplicate experiment.

4.10. In vivo anticancer activity

Six-week-old male BALB/c athymic nude mice with body weight of 18–20 g were used. A375 cancer cells (5×10^7 cells/mL in DMEM, 0.2 mL) were inoculated subcutaneously into the BALB/c nude mice. Treatment began when implanted tumors had reached a volume of 100-300 mm³ (7 days). All tumor-bearing mice were randomly divided into appropriate groups, with 6 mice in each group. Mice (n = 6 per group) were given **6f** (50 mg/kg, bid), vemurafenib (12.5 mg/kg, bid) and control (0.5% CMCNa) for 14 days by oral administration. Tumor volumes (calculated using the following formula, (width)² × length/2) and body weights were measured 2–3 times a week during the experiment. At the end of the experiment (at day 22), all mice were sacrificed and tumors were isolated and weighed.

4.11. Molecular docking simulation

The crystal structure of **NZT** with PKM2 (PDB 4G1N) was downloaded from protein databank (PDB: <http://www.rcsb.org>) and was prepared according to the Protein Preparation wizard in Maestro-Schrödinger suite 2016 (default values from the preprocess). The missing atoms appeared after this process and were completed using Prime. Moreover, hydrogen bonds assignment was optimized *via* Propka (pH = 7.0). Before docking process, the grid box was prepared according to the default size. LigPrep was used to predict ionization states for the ligands using a pH of 7.0 ± 2.0. In docking simulations using Glide, the protein was treated as rigid, compounds were

flexibly docked, and scoring was assigned according to the standard precision (SP) mode. Images depicting the proposed binding modes were generated using PyMOL software.

Acknowledgement

This work was supported by National Natural Science Foundation of China (No. 81673287, 21172011, 81502905)

References

- [1] W. Chen, R. Zheng, P.D. Baade, S. Zhang, H. Zeng, F. Bray, A. Jemal, X.Q. Yu, J. He, Cancer statistics in China, 2015, *CA Cancer J. Clin.* 66 (2016) 115-132.
- [2] D.A. Mahvi, R. Liu, M.W. Grinstaff, Y.L. Colson, C.P. Raut, Local cancer recurrence: The realities, challenges, and opportunities for new therapies, *CA Cancer J. Clin.* 68 (2018) 489-505.
- [3] R.L. Siegel, K.D. Miller, S.A. Fedewa, D.J. Ahnen, R.G.S. Meester, A. Barzi, A. Jemal, Colorectal cancer statistics, 2017, *CA Cancer J. Clin.* 67 (2017) 177-193.
- [4] K.S. Bhullar, N.O. Lagaron, E.M. McGowan, I. Parmar, A. Jha, B.P. Hubbard, H.P.V. Rupasinghe, Kinase-targeted cancer therapies: progress, challenges and future directions, *Mol. Cancer* 17 (2018) (article number: 48) 1-20.
- [5] F.M. Ferguson, N.S. Gray, Kinase inhibitors: the road ahead, *Nat. Rev. Drug Discov.* 17 (2018) 353-377.
- [6] Z.H. O'Brien, M.F. Moghaddam, A Systematic Analysis of Physicochemical and ADME Properties of All Small Molecule Kinase Inhibitors Approved by US FDA from January 2001 to October 2015, *Curr. Med. Chem.* 24 (2017) 3159-3184.
- [7] Y.P. Kang, N.P. Ward, G.M. DeNicola, Recent advances in cancer metabolism: a technological perspective, *Exp. Mol. Med.* 50 (2018) (article number: 31) 1-16.
- [8] U.E. Martinez-Outschoorn, M. Peiris-Pages, R.G. Pestell, F. Sotgia, M.P. Lisanti, Cancer metabolism: a therapeutic perspective, *Nat. Rev. Clin. Oncol.* 14 (2017)

11-31.

[9] M.G. Vander Heiden, Targeting cancer metabolism: a therapeutic window opens, *Nat. Rev. Drug Discov.* 10 (2011) 671-684.

[10] E.M. Stein, C.D. DiNardo, D.A. Pollyea, A.T. Fathi, G.J. Roboz, J.K. Altman, R.M. Stone, D.J. DeAngelo, R.L. Levine, I.W. Flinn, H.M. Kantarjian, R. Collins, M.R. Patel, A.E. Frankel, A. Stein, M.A. Sekeres, R.T. Swords, B.C. Medeiros, C. Willekens, P. Vyas, A. Tosolini, Q. Xu, R.D. Knight, K.E. Yen, S. Agresta, S. de Botton, M.S. Tallman, Enasidenib in mutant IDH2 relapsed or refractory acute myeloid leukemia, *Blood* 130 (2017) 722-731.

[11] O. Warburg, *Science* 123 (1956) 309-314.

[12] T. Noguchi, K. Yamada, H. Inoue, T. Matsuda, and T. Tanaka, The L- and R-type isozymes of rat pyruvate kinase are produced from a single gene by use of different promoters, *J. Biol. Chem.* 262 (1987) 14366-14371.

[13] B. Chaneton, E. Gottlieb, Rocking cell metabolism: revised functions of the key glycolytic regulator PKM2 in cancer, *Trends Biochem. Sci.* 37 (2012) 309-316.

[14] X. Gao, H. Wang, J.J. Yang, X. Liu, Z.R. Liu, Pyruvate kinase M2 regulates gene transcription by acting as a protein kinase, *Mol. Cell* 45 (2012) 598-609.

[15] W. Luo, H. Hu, R. Chang, J. Zhong, M. Knabel, R. O'Meally, R.N. Cole, A. Pandey, G.L. Semenza, Pyruvate kinase M2 is a PHD3-stimulated coactivator for hypoxia-inducible factor 1, *Cell* 145 (2011) 732-744.

[16] S. Mazurek, Pyruvate kinase type M2: a key regulator of the metabolic budget system in tumor cells, *Int. J. Biochem. Cell Biol.* 43 (2011) 969-980.

[17] H.P. Morgan, F.J. O'Reilly, M.A. Wear, J.R. O'Neill, L.A. Fothergill-Gilmore, T. Hupp, M.D. Walkinshaw, M2 pyruvate kinase provides a mechanism for nutrient sensing and regulation of cell proliferation, *Proc. Natl. Acad. Sci. (USA)* 110 (2013) 5881-5886.

[18] T. Hitosugi, S. Kang, M. G. Vander Heiden, T.W. Chung, S. Elf, K. Lythgoe, S. Dong, S. Lonial, X. Wang, G.Z. Chen, J. Xie, T.L. Gu, R.D. Polakiewicz, J.L. Roesel, T.J. Boggon, F.R. Khuri, D.G. Gilliland, L.C. Cantley, J. Kaufman, J. Chen, Tyrosine phosphorylation inhibits PKM2 to promote the Warburg effect and tumor growth, *Sci.*

Signal. 2 (2009) (article number: ra73) 1-10.

[19] W. Yang, Y. Xia, D. Hawke, X. Li, J. Liang, D. Xing, K. Aldape, T. Hunter, W.K. Alfred Yung, Z. Lu, PKM2 phosphorylates histone H3 and promotes gene transcription and tumorigenesis, *Cell* 150 (2012) 685-696.

[20] H.R. Christofk, M.G. Vander Heiden, M.H. Harris, A. Ramanathan, R.E. Gerszten, R. Wei, M.D. Fleming, S.L. Schreiber, L.C. Cantley, The M2 splice isoform of pyruvate kinase is important for cancer metabolism and tumour growth, *Nature* 452 (2008) 230-233.

[21] B. Chaneton, P. Hillmann, L. Zheng, A.C. Martin, O.D. Maddocks, A. Chokkathukalam, J.E. Coyle, A. Jankevics, F.P. Holding, K.H. Vousden, C. Frezza, M. O'Reilly, E. Gottlieb, Serine is a natural ligand and allosteric activator of pyruvate kinase M2, *Nature* 491 (2012) 458-462.

[22] W.J. Israelsen, M.G. Vander Heiden, Pyruvate kinase: Function, regulation and role in cancer, *Semin. Cell Dev. Biol.* 43 (2015) 43-51.

[23] S. Mazurek, C.B. Boschek, F. Hugo, E. Eigenbrodt, Pyruvate kinase type M2 and its role in tumor growth and spreading, *Semin. Cancer Biol.* 15 (2005) 300-308.

[24] S.L. Warner, K.J. Carpenter, D.J. Bearss, Activators of PKM2 in cancer metabolism, *Future Med. Chem.* 06 (2014) 1167-1178.

[25] S. Adem, A. Aslan, I. Ahmed, K. Krohn, C. Guler, V. Comakli, R. Demirdag, M. Kuzu, Inhibitory and Activating Effects of Some Flavonoid Derivatives on Human Pyruvate Kinase Isoenzyme M2, *Arch. Pharm.* 349 (2016) 132-136.

[26] D. Anastasiou, Y. Yu, W.J. Israelsen, J.K. Jiang, M.B. Boxer, B.S. Hong, W. Tempel, S. Dimov, M. Shen, A. Jha, H. Yang, K.R. Mattaini, C.M. Metallo, B.P. Fiske, K.D. Courtney, S. Malstrom, T.M. Khan, C. Kung, A.P. Skoumbourdis, H. Veith, N. Southall, M.J. Walsh, K.R. Brimacombe, W. Leister, S.Y. Lunt, Z.R. Johnson, K.E. Yen, K. Kunii, S.M. Davidson, H.R. Christofk, C.P. Austin, J. Inglese, M.H. Harris, J.M. Asara, G. Stephanopoulos, F.G. Salituro, S. Jin, L. Dang, D.S. Auld, H.W. Park, L.C. Cantley, C.J. Thomas, M.G. Vander Heiden, Pyruvate kinase M2 activators promote tetramer formation and suppress tumorigenesis, *Nat. Chem. Biol.* 8 (2012) 839-847.

- [27] M.B. Boxer, J.K. Jiang, M.G. Vander Heiden, M. Shen, A.P. Skoumbourdis, N. Southall, H. Veith, W. Leister, C.P. Austin, H.W. Park, J. Inglese, L.C. Cantley, D.S. Auld, C.J. Thomas, Evaluation of substituted N,N'-diarylsulfonamides as activators of the tumor cell specific M2 isoform of pyruvate kinase, *J. Med. Chem.* 53 (2010) 1048-1055.
- [28] C. Guo, A. Linton, M. Jalaie, S. Kephart, M. Ornelas, M. Pairish, S. Greasley, P. Richardson, K. Maegley, M. Hickey, J. Li, X. Wu, X. Ji, Z. Xie, Discovery of 2-((1H-benzo[d]imidazol-1-yl)methyl)-4H-pyrido[1,2-a]pyrimidin-4-ones as novel PKM2 activators, *Bioorg. Med. Chem. Lett.* 23 (2013) 3358-3363.
- [29] J.K. Jiang, M.B. Boxer, M.G. Vander Heiden, M. Shen, A.P. Skoumbourdis, N. Southall, H. Veith, W. Leister, C.P. Austin, H.W. Park, J. Inglese, L.C. Cantley, D.S. Auld, C.J. Thomas, Evaluation of thieno[3,2-b]pyrrole[3,2-d]pyridazinones as activators of the tumor cell specific M2 isoform of pyruvate kinase, *Bioorg. Med. Chem. Lett.* 20 (2010) 3387-3393.
- [30] D.J. Kim, Y.S. Park, N.D. Kim, S.H. Min, Y.M. You, Y. Jung, H. Koo, H. Noh, J.A. Kim, K.C. Park, Y.I. Yeom, A novel pyruvate kinase M2 activator compound that suppresses lung cancer cell viability under hypoxia, *Mol. Cells* 38 (2015) 373-379.
- [31] C. Kung, J. Hixon, S. Choe, K. Marks, S. Gross, E. Murphy, B. DeLaBarre, G. Cianchetta, S. Sethumadhavan, X. Wang, S. Yan, Y. Gao, C. Fang, W. Wei, F. Jiang, S. Wang, K. Qian, J. Saunders, E. Driggers, H.K. Woo, K. Kunii, S. Murray, H. Yang, K. Yen, W. Liu, L.C. Cantley, M.G. Vander Heiden, S.M. Su, S. Jin, F.G. Salituro, L. Dang, Small molecule activation of PKM2 in cancer cells induces serine auxotrophy, *Chem. Biol.* 19 (2012) 1187-1198.
- [32] R. Li, X. Ning, S. Zhou, Z. Lin, X. Wu, H. Chen, X. Bai, X. Wang, Z. Ge, R. Li, Y. Yin, Discovery and structure-activity relationship of novel 4-hydroxy-thiazolidine-2-thione derivatives as tumor cell specific pyruvate kinase M2 activators, *Eur. J. Med. Chem.* 143 (2018) 48-65.
- [33] Y. Matsui, I. Yasumatsu, T. Asahi, T. Kitamura, K. Kanai, O. Ubukata, H. Hayasaka, S. Takaishi, H. Hanzawa, S. Katakura, Discovery and structure-guided

fragment-linking of 4-(2,3-dichlorobenzoyl)-1-methyl-pyrrole-2-carboxamide as a pyruvate kinase M2 activator, *Bioorg. Med. Chem.* 25 (2017) 3540-3546.

[34] K.M. Parnell, J.M. Foulks, R.N. Nix, A. Clifford, J. Bullough, B. Luo, A. Senina, D. Vollmer, J. Liu, V. McCarthy, Y. Xu, M. Saunders, X.H. Liu, S. Pearce, K. Wright, M. O'Reilly, M.V. McCullar, K.K. Ho, S.B. Kanner, Pharmacologic activation of PKM2 slows lung tumor xenograft growth, *Mol. Cancer Ther.* 12 (2013) 1453-1460.

[35] M.J. Walsh, K.R. Brimacombe, H. Veith, J.M. Bougie, T. Daniel, W. Leister, L.C. Cantley, W.J. Israelsen, M.G. Vander Heiden, M. Shen, D.S. Auld, C.J. Thomas, M.B. Boxer, 2-Oxo-N-aryl-1,2,3,4-tetrahydroquinoline-6-sulfonamides as activators of the tumor cell specific M2 isoform of pyruvate kinase, *Bioorg. Med. Chem. Lett.* 21 (2011) 6322-6327.

[36] Y. Xu, X.H. Liu, M. Saunders, S. Pearce, J.M. Foulks, K.M. Parnell, A. Clifford, R.N. Nix, J. Bullough, T.F. Hendrickson, K. Wright, M.V. McCullar, S.B. Kanner, K.K. Ho, Discovery of 3-(trifluoromethyl)-1H-pyrazole-5-carboxamide activators of the M2 isoform of pyruvate kinase (PKM2), *Bioorg. Med. Chem. Lett.* 24 (2014) 515-519.

[37] A. Yacovan, R. Ozeri, T. Kehat, S. Mirilashvili, D. Sherman, A. Aizikovich, A. Shitrit, E. Ben-Zeev, N. Schutz, O. Bohana-Kashtan, A. Konson, V. Behar, O.M. Becker, 1-(sulfonyl)-5-(arylsulfonyl)indoline as activators of the tumor cell specific M2 isoform of pyruvate kinase, *Bioorg. Med. Chem. Lett.* 22 (2012) 6460-6468.

[38] J. Li, S. Li, J. Guo, Q. Li, J. Long, C. Ma, Y. Ding, C. Yan, L. Li, Z. Wu, H. Zhu, K.K. Li, L. Wen, Q. Zhang, Q. Xue, C. Zhao, N. Liu, I. Ivanov, M. Luo, R. Xi, H. Long, P.G. Wang, Y. Chen, Natural Product Micheliolide (MCL) Irreversibly Activates Pyruvate Kinase M2 and Suppresses Leukemia, *J. Med. Chem.* 61 (2018) 4155-4164.

[39] Y. Zhang, B. Liu, X. Wu, R. Li, X. Ning, Y. Liu, Z. Liu, Z. Ge, R. Li, Y. Yin, New pyridin-3-ylmethyl carbamodithioic esters activate pyruvate kinase M2 and potential anticancer lead compounds, *Bioorg. Med. Chem.* 23 (2015) 4815-4823.

[40] Y. Ohshiro, M. Komatsu, S. Minakata, Regioselective functionalization of

- 1H-pyrrolo[2,3-b]pyridine *via* its N-oxide, *Synthesis* 24 (1992) 661-663.
- [41] Y.S. Tung, M.S. Coumar, Y.S. Wu, H.Y. Shiao, J.Y. Chang, J.P. Liou, P. Shukla, C.W. Chang, C.Y. Chang, C.C. Kuo, T.K. Yeh, C.Y. Lin, J.S. Wu, S.Y. Wu, C.C. Liao, H.P. Hsieh, Scaffold-hopping strategy: synthesis and biological evaluation of 5,6-fused bicyclic heteroaromatics to identify orally bioavailable anticancer agents, *J. Med. Chem.* 54 (2011) 3076-3080.
- [42] F.X. Tavares, J.A. Boucheron, S.H. Dickerson, R.J. Griffin, F. Preugschat, S.A. Thomson, T.Y. Wang, H.Q. Zhou, N-Phenyl-4-pyrazolo[1,5-b]pyridazin-3-ylpyrimidin-2-amines as Potent and Selective Inhibitors of Glycogen Synthase Kinase 3 with Good Cellular Efficacy, *J. Med. Chem.* 47 (2004) 4716-4730.
- [43] S. Patnaik, H.C. Dietz, W. Zheng, C. Austin, J.J. Marugan, Multi-gram scale synthesis of FR180204, *J. Org. Chem.* 74 (2009) 8870-8873.
- [44] J. Liang, R. Cao, Y. Zhang, Y. Xia, Y. Zheng, X. Li, L. Wang, W. Yang, Z. Lu, PKM2 dephosphorylation by Cdc25A promotes the Warburg effect and tumorigenesis, *Nat. Commun.* 7 (2016) (article number: 12431) 1-13.
- [45] W. Yang, Y. Xia, H. Ji, Y. Zheng, J. Liang, W. Huang, X. Gao, K. Aldape, Z. Lu, Nuclear PKM2 regulates beta-catenin transactivation upon EGFR activation, *Nature* 480 (2011) 118-122.
- [46] W. Yang, Y. Zheng, Y. Xia, H. Ji, X. Chen, F. Guo, C.A. Lyssiotis, K. Aldape, L.C. Cantley, Z. Lu, ERK1/2-dependent phosphorylation and nuclear translocation of PKM2 promotes the Warburg effect, *Nat. Cell Biol.* 14 (2012) 1295-1304.
- [47] W. Yang, Z. Lu, Regulation and function of pyruvate kinase M2 in cancer, *Cancer Lett.* 339 (2013) 153-158.
- [48] R.A. Harris, A.W. Fenton, A critical review of the role of M2PYK in the Warburg effect, *BBA-Rev. Cancer* 1871 (2019) 225-239.
- [49] S.T. Sizemore, M. Zhang, J.H. Cho, G.M. Sizemore, B. Hurwitz, B. Kaur, N.L. Lehman, M.C. Ostrowski, P.A. Robe, W. Miao, Y. Wang, A. Chakravarti, F. Xia, Pyruvate kinase M2 regulates homologous recombination-mediated DNA double-strand break repair, *Cell Res.* 28 (2018) 1090-1102.

- [50] M.S. Goldberg, P.A. Sharp, Pyruvate kinase M2-specific siRNA induces apoptosis and tumor regression, *J. Exp. Med.* 209 (2012) 217-224.
- [51] G. Prakasam, R.K. Singh, M.A. Iqbal, S.K. Saini, A.B. Tiku, R.N.K. Bamezai, Pyruvate kinase M knockdown-induced signaling via AMP-activated protein kinase promotes mitochondrial biogenesis, autophagy, and cancer cell survival, *J. Biol. Chem.* 292 (2017) 15561-15576.
- [52] C. Wang, J. Jiang, J. Ji, Q. Cai, X. Chen, Y. Yu, Z. Zhu, J. Zhang, PKM2 promotes cell migration and inhibits autophagy by mediating PI3K/AKT activation and contributes to the malignant development of gastric cancer, *Sci. Rep.* 7 (2017) (article number: 2886) 1-14.
- [53] G. Qian, X. Hong, B. Liu, H. Mao, B. Xu, Rhodium-catalyzed regioselective C-H chlorination of 7-azaindoles using 1,2-dichloroethane, *Org. Lett.* 16 (2014) 5294-5297.
- [54] M.P. Huestis, K. Fagnou, Site-Selective Azaindole Arylation at the Azine and Azole Rings *via* N-Oxide Activation, *Org. Lett.* 11 (2009) 1357-1360.
- [55] G. Chen, H. Ren, N. Zhang, W. Lennox, A. Turpoff, S. Paget, C. Li, N. Almstead, F.G. Njoroge, Z. Gu, J. Graci, S.P. Jung, J. Colacino, F. Lahser, X. Zhao, M. Weetall, A. Nomeir, G.M. Karp, 6-(Azaindol-2-yl)pyridine-3-sulfonamides as potent and selective inhibitors targeting hepatitis C virus NS4B, *Bioorg. Med. Chem. Lett.* 25 (2015) 781-786.
- [56] B. Liu, X. Wang, Z.M. Ge, R.T. Li, Regioselective Ir(III)-catalyzed C-H alkynylation directed by 7-azaindoles, *Org. Biomol. Chem.* 14 (2016) 2944-2949.

Highlights:

- Novel 7-azaindole derivatives containing pyridin-3-ylmethyl dithiocarbamate moiety were optimized as potent PKM2 activators.
- Compound **6f** has great anti-proliferation activities on A375 cell lines both *in vitro* and *in vivo*.
- Compound **6f** could influence the translocation of PKM2 into nucleus, as well as induction of apoptosis and autophagy on A375 cells.
- Compound **6f** could efficiently exhibit antimetastatic potential against cancer cells.